

Cronin Effect and High- p_T Suppression in pA Collisions

Dmitri Kharzeev¹, Yuri V. Kovchegov² and Kirill Tuchin³

¹ *Nuclear Theory Group, Brookhaven National Laboratory, Bldg. 510A
Upton, NY 11973*

² *Department of Physics, University of Washington, Box 351560
Seattle, WA 98195*

³ *Institute for Nuclear Theory, University of Washington, Box 351550
Seattle, WA 98195*

We review the predictions of the theory of Color Glass Condensate for gluon production cross section in p(d)A collisions. We demonstrate that at moderate energies, when the gluon production cross section can be calculated in the framework of McLerran-Venugopalan model, it has only partonic level Cronin effect in it. At higher energies/rapidities corresponding to smaller values of Bjorken x quantum evolution becomes important. The effect of quantum evolution is to introduce suppression of gluons produced at high- p_T without removing the Cronin effect.

I. INTRODUCTION

Recently there has been a surge of interest in particle production in proton-nucleus (pA) and deuteron-nucleus (dA) collisions at high energies. The interest was inspired by the new data produced by the dA program at RHIC [1–3], which should enable one to separate the contributions of the initial state effects [7] such as parton saturation [8–12] from the final state effects, such as jet quenching and energy loss in the quark-gluon plasma (QGP) [13–16], to the suppression of high transverse momentum particles observed in $Au - Au$ collisions at RHIC [4–6].

Saturation physics has been largely successful in describing hadron multiplicities in Au-Au collisions at RHIC [17]. It can also have important implications for the transverse momentum distributions [18] and particle correlations and azimuthal anisotropies [19]. It has been demonstrated [20] that saturation provides very favorable initial conditions for the thermalization of parton modes with the transverse momenta $k_T \sim Q_s$, where Q_s is the saturation scale. The thermalization was also found [20] to approximately preserve the centrality dependence of total hadron multiplicities determined by the initial conditions [17]. Recent lattice results [21,22] show that the initial average transverse momentum $\langle k_T \rangle$ of the produced partons is $\langle k_T \rangle \sim Q_s$, which makes the “soft thermalization” scenario preserving the initial centrality and rapidity distributions quite likely. Final state interactions, however, will undoubtedly modify the transverse momentum distributions at $k_T \leq (1 \div 3) Q_s$ without introducing new momentum scale [20]. If the produced medium lives long enough, then high k_T jets will be suppressed as well because of the jet quenching and energy loss [13–16].

The first $d - Au$ data from RHIC show Cronin enhancement extending up to $k_T \simeq 6$ GeV around $y \sim 0$ [1,3] whereas at slightly forward rapidity around $y \sim 1$ no significant enhancement is seen [2]. The absence

of suppression indicates that final state interactions are indeed responsible for the effect observed in $Au - Au$ collisions [4–6] in the same k_T range. The non-universality of the ratios for the charged hadron and π^0 spectra [1] however indicates deviations from the independent jet fragmentation up to $k_T \simeq 5$ GeV. It remains to be checked if there is a suppression of high k_T charged hadron and π^0 yields above the Cronin enhancement region ($k_T \geq 6$ GeV), and if this suppression depends on centrality of $d - Au$ collisions. This question is of crucial importance for the interpretation of the spectacular effect observed in $Au - Au$ collisions [4–6] because this is the kinematical region in which the independent jet fragmentation picture, and thus the perturbative jet quenching description, begin to apply.

The first dA data from RHIC [1–3] give the ratio of the number of particles produced in a dA collision over the number of particles produced in a pp collision scaled by the number of collisions

$$R^{dA}(k_T, y) = \frac{\frac{dN^{dA}}{d^2k dy}}{N_{coll} \frac{dN_{pp}}{d^2k dy}}. \quad (1)$$

To understand the new data on R^{dA} and what it implies for our understanding of high energy nuclear wave functions we are going to study here the expectations for R^{dA} from saturation physics. Our approach will be somewhat academic: in this paper, we will not include explicitly all of the effects related to the fact that high- k_T of produced particles corresponds to rather large Bjorken x in the actual RHIC experiments at central rapidity – the effective Bjorken x of high- k_T ($k_T > 5$ GeV) particles observed at mid-rapidity at RHIC at $\sqrt{s} = 200$ GeV is about $x \approx 0.1$ which may be too large for the small- x treatment that we present here (see [23], but see also [24]). These finite-energy effects have to be accurately accounted for before we can compare our calculations to the data. Nevertheless, we feel that a better understanding of the qualitative features of hadron production within the saturation framework is a necessary pre-requisite for a complete theoretical description of high energy $p(d) - A$ collisions.

We assume that collisions take place at very high energy such that the effective Bjorken x is sufficiently small for all k_T of interest. For simplicity we will analyze proton-nucleus collisions assuming that the main qualitative conclusions would be applicable to dA. Since we can not calculate N_{coll} in a model-independent way, we will be using Eq. (25) for our definition of R^{pA} , which is identical to Eq. (1) applied to pA collisions with a proper definition of N_{coll} (see [25] for a discussion of uncertainties involved in theoretical evaluations of this quantity).

The problem of gluon production in pA collisions has been solved in the framework of McLerran-Venugopalan model [11] in [26] (see also [27–30]). The resulting cross section includes the effects of all multiple rescatterings of the produced gluon and the proton in the target nucleus [26]. At higher energy quantum evolution becomes important [31–38]. In the large N_c limit the small- x evolution equation can be written in a non-linear integro-differential form [32–35] shown here in Eq. (41). The inclusion of non-linear evolution [32–35] in the quasi-classical gluon production cross section of [26] has been done in [39] (see also [40,41]). The study of the resulting gluon spectrum and corresponding gluonic R^{pA} is the goal of this paper.

The paper is organized as follows. In Sect. IIA we discuss two main definitions of unintegrated gluon distribution functions: the standard definition (2) and the one inspired by non-Abelian Weizsäcker-Williams field of a nucleus in McLerran-Venugopalan model (6) [11,12]. We argue, following [39,42], that the Eq. (6) is the correct definition of the unintegrated gluon distribution counting the number of gluon quanta. We proceed in Sect. IIB by proving the sum rules for both distribution functions given in Eqs. (12) and (13). The sum rules insure that the presence of shadowing in nuclear gluon distribution functions in the saturation regime ($k_T \lesssim Q_{s0}$) require enhancement of gluons at higher k_T ($k_T \gtrsim Q_{s0}$) reminiscent of anti-shadowing. In Sect. IIC this conclusion is quantified in the framework of McLerran-Venugopalan model of multiple rescatterings [11,43] [see Fig. 3 and Eqs. (21) and (22)].

In Sect. III we apply the developed techniques to the gluon production cross section in pA. In Sect. IIIA we show that the gluon production cross section calculated in [26] in McLerran-Venugopalan multiple rescattering model exhibits only Cronin-like enhancement [44], as shown in Fig. 4 and in Eq. (30) (cf. [45,46]). We proceed in Sect. IIIB by proving a sum rule (38) which insures that suppression of produced gluons at low k_T ($k_T \lesssim Q_{s0}$) demands Cronin-like enhancement at high k_T ($k_T \gtrsim Q_{s0}$). The relative amounts of suppression and enhancement are different from the gluon distribution case of Sect. II. We also point out that, surprisingly the gluon production cross section in pA can be written in a k_T -factorized form (35) [8,47] with the unintegrated distribution functions defined by Eq. (2), physical meaning of which is less clear than that of Weizsäcker-Williams ones (6).

Sect. IV is devoted to studying the effects of nonlinear evolution (41) on the gluon production cross section in pA. In Sect. IVA we use the analogy to the case of gluon production in deep inelastic scattering (DIS) solved in [39,41] to include the effects of evolution (41) in the gluon production cross section in pA. The result is given by Eq. (45). By expanding the all-twist formula (45) we then study the effect of nonlinear evolution on the gluon production at the leading twist (Sect. IVB) and next-to-leading twist (Sect. IVC) level. In Sect. IVB we start by deriving gluon production cross section at the leading twist level (55). We then estimate the cross section for high k_T ($k_T \gg Q_s(y)$) in the double logarithmic approximation (59) [47] and demonstrate that the corresponding R^{pA} is approaching 1 at high k_T from below, i.e., that $R^{pA} < 1$ at $k_T \gg Q_s(y)$. We proceed by evaluating Eq. (55) in the extended geometric scaling region ($Q_s(y) < k_T \lesssim k_{\text{geom}}$) [42,48,49]. The resulting leading twist gluon production cross section (79) leads to further suppression of gluon production due to the change in gluon anomalous dimension [7] as shown in Eqs. (82) and (84). The next-to-leading twist contribution to the gluon production cross section in pA is evaluated in Sect. IVC with the result given by Eq. (90). One can see that the subleading twist contribution brings in extra suppression at high k_T ($k_T \sim k_{\text{geom}}$) and contributes towards the onset of Cronin enhancement at lower k_T ($k_T \sim Q_s(y)$). In Sect. IVD we construct a toy model illustrating our conclusion that at high enough energy the effect of nonlinear evolution (41) is to introduce suppression of high k_T gluons *without* eliminating Cronin enhancement, as shown in Fig. 8. We conclude in Sect. V by summarizing our results.

II. A TALE OF TWO GLUON DISTRIBUTION FUNCTIONS

A. Definitions

There are two different ways to define unintegrated gluon distribution function of a proton or nucleus. The most conventional way relates it to the $q\bar{q}$ dipole cross section on the target nucleus via two gluon exchange. Here we are going to use a similar definition relating the unintegrated gluon distribution to the dipole cross section on the nucleus (see Fig. 1).

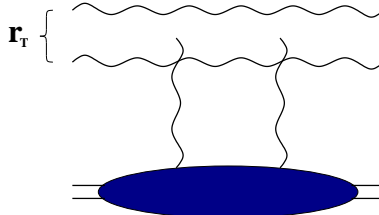


FIG. 1. “Conventional” definition of unintegrated gluon distribution relating it to the gluon dipole cross section. The exchanged gluon lines can connect to either gluon in the dipole.

The corresponding gluon distribution is given by (cf. [38,40])

$$\phi(x, \underline{k}^2) = \frac{C_F}{\alpha_s (2\pi)^3} \int d^2 b d^2 r e^{-i \underline{k} \cdot \underline{r}} \nabla_r^2 N_G(\underline{r}, \underline{b}, y = \ln 1/x), \quad (2)$$

where $N_G(\underline{r}, \underline{b}, y = \ln 1/x)$ is the forward amplitude of a gluon dipole of transverse size \underline{r} at impact parameter \underline{b} and rapidity y scattering on a nucleus [32,39]. We denote by \underline{k} the transverse components of the four-vector k , and by k_T its length. The definition of Eq. (2) is inspired by k_T -factorization and is valid as long as one can neglect multiple rescatterings of the dipole in the nucleus. By using Eq. (2) in the saturation region where higher twists (multiple rescatterings) become important one implicitly assumes that there exists a certain gauge in which the $q\bar{q}$ dipole cross section on a nucleus is given by a two gluon exchange interaction between the dipole and the nucleus and the interaction shown in Fig. 1 is literally all one needs to obtain the correct dipole cross section. It is not clear at present whether this is the case and such a gauge exists. Therefore the gluon distribution given by Eq. (2) does not give one the number of gluons in the nuclear wave function in the saturation region. The applications of the definition (2) will be clarified later.

Another definition of unintegrated gluon distribution literally counts the number of gluons in the nuclear wave function. To construct it in the quasi-classical limit of high energy QCD given by McLerran-Venugopalan model [11] one has to first find the classical gluonic field of the nucleus in the light cone gauge of the ultrarelativistic nucleus (non-Abelian Weizsäcker-Williams field) and then calculate the correlator of two of such fields to get unintegrated gluon distribution function (see Fig. 2).

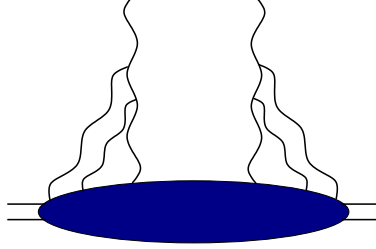


FIG. 2. Definition of unintegrated gluon distribution in McLerran-Venugopalan model.

The non-Abelian Weizsäcker-Williams field of a nucleus has been found in [12], leading to the following expression for the corresponding gluon distribution [12,26]

$$\begin{aligned}\phi^{WW}(x, \underline{k}^2) &= \frac{1}{2\pi^2} \int d^2b d^2r e^{-i\underline{k}\cdot\underline{r}} \text{Tr} \langle \underline{A}^{WW}(\underline{0}) \cdot \underline{A}^{WW}(\underline{r}) \rangle \\ &= \frac{4C_F}{\alpha_s (2\pi)^3} \int d^2b d^2r e^{-i\underline{k}\cdot\underline{r}} \frac{1}{\underline{r}^2} (1 - e^{-\underline{r}^2 Q_{s0}^2 \ln(1/r_T \Lambda)/4}),\end{aligned}\quad (3)$$

where

$$Q_{s0}^2(\underline{b}) = 4\pi \alpha_s^2 \rho T(\underline{b}), \quad (4)$$

with ρ the atomic number density in the nucleus with atomic number A , $T(\underline{b})$ the nuclear profile function and Λ some infrared cutoff.

Generalizing Eq. (3) to include non-linear small- x evolution in it [32–35] is rather difficult. However, the problem of including small- x evolution has been solved for F_2 structure function and for the gluon production cross section in DIS [32,39]. Inspired by those examples we conjecture that replacing the Glauber-Mueller [43] forward gluon dipole amplitude on the nucleus by its' fully evolved expression to be found from the nonlinear evolution equation [32,35]

$$1 - e^{-\underline{r}^2 Q_{s0}^2 \ln(1/r_T \Lambda)/4} \Rightarrow N_G(\underline{r}, \underline{b}, y) \quad (5)$$

would give us the unintegrated gluon distribution function of a nucleus in the general case:

$$\phi^{WW}(x, \underline{k}^2) = \frac{4C_F}{\alpha_s (2\pi)^3} \int d^2b d^2r e^{-i\underline{k}\cdot\underline{r}} \frac{1}{\underline{r}^2} N_G(\underline{r}, \underline{b}, y = \ln 1/x). \quad (6)$$

Similar expression for gluon distribution was obtained earlier in [42].

An important observation concerning the two gluon distributions presented above has been made in [39,40]. It was shown that, while the Weizsäcker-Williams gluon distribution of Eq. (6) indeed has a clear physical meaning of counting the number of gluons [12], it is the gluon distribution inspired by k_T -factorization and given by Eq. (2) that enters gluon production cross section in pA collisions and in DIS [39,40]. More precisely, the gluon production cross section including the effects of multiple rescatterings and quantum evolution in it can be reduced to a k_T -factorized form [8] with the unintegrated gluon distribution of a nucleus given by Eq. (2) [39]. The authors can not offer any simple physical explanation of this paradox. Nevertheless we keep both distributions in the discussion below keeping in mind that the first one is more relevant to particle production in pA.

B. k_T -dependence: General Arguments

Both definitions of unintegrated gluon distribution (2) and (6) have the same high- k_T asymptotic, which in the quasi-classical approximation (see e.g. Eq. (3)) reads

$$\phi_A(x, \underline{k}^2) = \phi_A^{WW}(x, \underline{k}^2) = A \phi_N(x, \underline{k}^2) = A \frac{\alpha_s C_F}{\pi} \frac{1}{\underline{k}^2}, \quad k_T \rightarrow \infty, \quad (7)$$

where the index A (N) denotes gluon distribution in a nucleus (nucleon). Therefore the distributions are equivalent at the level of leading twist, i.e., as long as we include only a single rescattering in the dipole amplitude N_G .

Both gluon distributions obey a sum rule which we are going to prove here for ϕ^{WW} . From Eq. (6) one can easily infer that

$$\int d^2k \phi_A^{WW}(x, \underline{k}^2) = \frac{4 C_F}{\alpha_s (2\pi)} \int d^2b \left(\frac{1}{\underline{r}^2} N_G(\underline{r}, \underline{b}, y = \ln 1/x) \right) \Big|_{\underline{r}=0}. \quad (8)$$

At very small r_T the dipole cross section N_G goes to zero as r_T^2 (color transparency [50]) with the coefficient in the front proportional to $A^{1/3}$. One can see that this is explicitly true for the Glauber-Mueller expression for the dipole cross section N_G [43]

$$N_G(\underline{r}, \underline{b}, y = 0) = 1 - e^{-\underline{r}^2 Q_{s0}^2 \ln(1/r_T \Lambda)/4}. \quad (9)$$

At extremely small r_T the dipole cross section N_G would loose all the effects of the small- x evolution and reduce to the equation's initial condition given for N_G by Eq. (9). Thus we can always write

$$\left(\frac{1}{\underline{r}^2} N_G(\underline{r}, \underline{b}, y = \ln 1/x) \right) \Big|_{\underline{r}=0} = A^{1/3} \left(\frac{1}{\underline{r}^2} n_G(\underline{r}, \underline{b}, y = \ln 1/x) \right) \Big|_{\underline{r}=0}, \quad (10)$$

where n is the dipole cross section on a single nucleon N . Remembering that

$$\int_A d^2b = A^{2/3} \int_N d^2b \quad (11)$$

we conclude from Eq. (8) that (see also [26])

$$\int d^2k \phi_A^{WW}(x, \underline{k}^2) = A \int d^2k \phi_N^{WW}(x, \underline{k}^2). \quad (12)$$

Similarly one can show that the k_T -factorization gluon distribution Eq. (2) obeys the same sum rule

$$\int d^2k \phi_A(x, \underline{k}^2) = A \int d^2k \phi_N(x, \underline{k}^2). \quad (13)$$

The sum rule of Eqs. (12) and (13) implies that at some k_T the distribution function $\phi_A^{WW}(x, \underline{k}^2)$ is smaller than $A \phi_N^{WW}(x, \underline{k}^2)$, then at some other k_T it should be bigger than $A \phi_N^{WW}(x, \underline{k}^2)$. If one defines the unintegrated gluon distributions ratio as

$$R_A(x, \underline{k}^2) = \frac{\phi_A(x, \underline{k}^2)}{A \phi_N(x, \underline{k}^2)} \quad \text{and} \quad R_A^{WW}(x, \underline{k}^2) = \frac{\phi_A^{WW}(x, \underline{k}^2)}{A \phi_N^{WW}(x, \underline{k}^2)} \quad (14)$$

one concludes from Eq. (12) that if R_A^{WW} is below 1 at some k_T it is bound to go above 1 at some other k_T (for the same value of x). From Eq. (7) we can conclude that

$$R_A^{WW}(x, \underline{k}^2), R_A(x, \underline{k}^2) \rightarrow 1, \quad k_T \rightarrow \infty. \quad (15)$$

At the same time, when $k_T \ll Q_{s0}$ the saturation effects become important driving $\phi_A^{WW}(x, \underline{k}^2)$ below $A\phi_N^{WW}(x, \underline{k}^2)$, or, equivalently, making $R_A^{WW}(x, \underline{k}^2) < 1$. Therefore, due to the sum rule of Eqs. (12) and (13), somewhere in the region of $k_T \gtrsim Q_{s0}$ the ratio $R_A^{WW}(x, \underline{k}^2)$ should go above one, which corresponds to enhancement or broadening of the k_T distribution of gluons inside the nucleus. The same broadening argument applies to $\phi_A(x, \underline{k}^2)$. We have therefore proved that for both gluon distribution functions the effects of saturation and the sum rule (12),(13), while making $R_A(x, \underline{k}^2) < 1$ in deep infrared, also require an existence of a k_T -region where $R_A(x, \underline{k}^2)$ is above 1. This conclusion is independent of the model one takes for the dipole amplitude N_G : it is valid for Glauber-Mueller multiple rescatterings as well as for small- x evolution of Eq. (41).

C. k_T -dependence: Quasi-Classical Approximation

To investigate the k_T -dependence of the unintegrated nuclear gluon distributions $\phi_A^{WW}(x, \underline{k}^2)$ and $\phi_A(x, \underline{k}^2)$ more quantitatively and demonstrate the differences of the two distributions let us study them in McLerran-Venugopalan model [11,12]. For that we take the gluon dipole amplitude in the Glauber-Mueller approximation [43] of Eq. (9). The high- k_T asymptotic for both $\phi_A^{WW}(x, \underline{k}^2)$ and $\phi_A(x, \underline{k}^2)$ is given by Eq. (7).

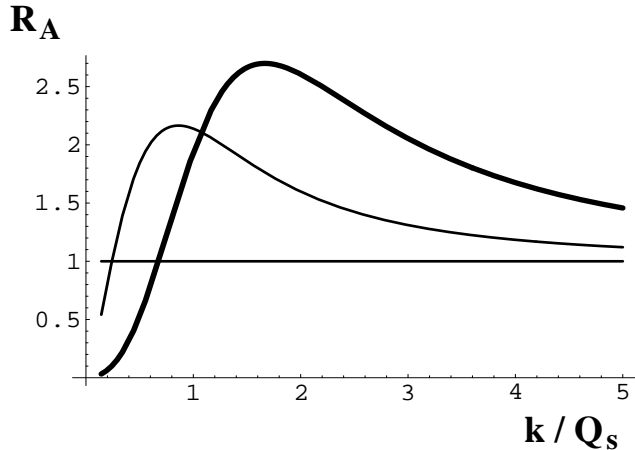


FIG. 3. The ratio R_A of unintegrated gluon distributions in the nucleus and in the nucleon. The thin line represents the Weizsäcker-Williams gluon distribution [Eq. (6)] while the thick line correspond to the more conventional one inspired by k_T -factorization [Eq. (2)].

Inside the saturation region ($k_T \ll Q_{s0}$) one has

$$\phi(x, \underline{k}^2) \approx \frac{2 C_F S_A}{\alpha_s (2\pi)^2} \frac{k_T^2}{Q_{s0}^2}, \quad k_T \ll Q_{s0}, \quad (16)$$

and

$$\phi^{WW}(x, \underline{k}^2) \approx \frac{4 C_F S_A}{\alpha_s (2\pi)^2} \ln \frac{Q_{s0}}{k_T}, \quad k_T \ll Q_{s0}, \quad (17)$$

where we assumed for simplicity that the nucleus is cylindrical in which case its cross sectional area is $S_A = \pi \mathcal{R}^2$ and Q_{s0} is given by Eq. (4) with $\rho T(\underline{b}) = A/S_A$:

$$Q_{s0}^2 = \frac{4\pi \alpha_s^2 A}{S_A}, \quad \text{cylindrical nucleus.} \quad (18)$$

In Eqs. (16) and (17) the difference between the two gluon distribution functions becomes manifest: $\phi_A^{WW}(x, \underline{k}^2)$ keeps increasing (though only logarithmically) as k_T decreases, while $\phi_A(x, \underline{k}^2)$ turns over and goes to zero in the infrared. Still for both distribution functions the ratio R_A goes to zero as $k_T \rightarrow 0$ since

to obtain R_A one has to divide Eqs. (16) and (17) by $A\phi_N(x, \underline{k}^2)$ from Eq. (7). The sum rules (12) and (13) require a region of enhancement ($R_A > 1$) at $k_T \gtrsim Q_{s0}$. To see that the enhancement really happens one has to calculate the next-to-leading twist correction to the high- k_T asymptotic of Eq. (7). This technique has been applied previously for quark production in [51]. One obtains

$$\phi_A(x, \underline{k}^2) = \frac{C_F S_A Q_{s0}^2}{\alpha_s (2\pi)^2 \underline{k}^2} \left[1 + 2 \frac{Q_{s0}^2}{\underline{k}^2} \left(\ln \frac{\underline{k}^2}{4\Lambda^2} + 2\gamma - 3 \right) + \dots \right], \quad k_T \rightarrow \infty, \quad (19)$$

and

$$\phi_A^{WW}(x, \underline{k}^2) = \frac{C_F S_A Q_{s0}^2}{\alpha_s (2\pi)^2 \underline{k}^2} \left[1 + \frac{Q_{s0}^2}{\underline{k}^2} \left(\ln \frac{k_T}{2\Lambda} + \gamma - 1 \right) + \dots \right], \quad k_T \rightarrow \infty, \quad (20)$$

with γ the Euler constant. For the ratios R_A 's this implies

$$R_A = 1 + 2 \frac{Q_{s0}^2}{\underline{k}^2} \left(\ln \frac{\underline{k}^2}{4\Lambda^2} + 2\gamma - 3 \right) + \dots \quad (21)$$

and

$$R_A^{WW} = 1 + \frac{Q_{s0}^2}{\underline{k}^2} \left(\ln \frac{k_T}{2\Lambda} + \gamma - 1 \right) + \dots \quad (22)$$

Therefore the ratios of gluon distributions approach 1 from above for both distribution functions at large k_T . This of course indicates the presence of high- k_T enhancement.

Qualitative plots of ratio R_A for both distribution functions in McLerran-Venugopalan model are shown in Fig. 3. The thin line corresponds to Weizsäcker-Williams gluon distribution $\phi_A^{WW}(x, \underline{k}^2)$ while the thick one represents the k_T -factorization distribution $\phi_A(x, \underline{k}^2)$. One can see that in accordance with Eqs. (16) and (17) the distribution $\phi_A(x, \underline{k}^2)$ goes to zero faster than $\phi_A^{WW}(x, \underline{k}^2)$ as $k_T \rightarrow 0$ in Fig. 3. In agreement with Eqs. (22) and (21) R_A for the distribution $\phi_A(x, \underline{k}^2)$ has a stronger high- k_T enhancement than R_A^{WW} for the distribution $\phi_A^{WW}(x, \underline{k}^2)$.

Finally, let us point out that the suppression in R_A (R_A^{WW}) introduced by saturation physics at small k_T together with the sum rule of Eqs. (12) and (13) does not necessarily rule out a possibility of high- k_T suppression. One can imagine a gluon distribution giving R_A that still goes below 1 at $k_T \lesssim Q_s$, than becomes greater than 1 at some intermediate k_T and still dives under 1 at high k_T . This is not the case for the gluon distributions in the quasi-classical approximation considered in Fig. 3. However, as we will see below in Sect. IV the effects of quantum evolution are likely to modify the distribution functions introducing the high k_T suppression.

III. QUASI-CLASSICAL APPROXIMATION: CRONIN EFFECT ONLY

A. Gluon Production in pA

The problem of gluon production in proton-nucleus collisions in the quasi-classical approximation (McLerran-Venugopalan model) has been solved in [26] (see also [27,30,28,29]). For a quark-nucleus scattering the production cross section reads [26]

$$\frac{d\sigma^{pA}}{d^2k dy} = \int d^2b d^2x d^2y \frac{1}{(2\pi)^2} \frac{\alpha_s C_F}{\pi^2} \frac{\underline{x} \cdot \underline{y}}{\underline{x}^2 \underline{y}^2} e^{-i\underline{k} \cdot (\underline{x} - \underline{y})} \times \left(1 - e^{-\underline{x}^2 Q_{s0}^2 \ln(1/x_T \Lambda)/4} - e^{-\underline{y}^2 Q_{s0}^2 \ln(1/y_T \Lambda)/4} + e^{-(\underline{x} - \underline{y})^2 Q_{s0}^2 \ln(1/(\underline{x} - \underline{y})_T \Lambda)/4} \right), \quad (23)$$

which then has to be convoluted with the light cone wave function of a quark in a proton. The saturation scale Q_{s0}^2 in Eq. (23) is given by Eq. (4). As was shown in [26] in the approximation when the logarithmic

dependence of exponential factors in Eq. (23) on the transverse size is neglected, $\underline{x}^2 \ln(1/x_T \Lambda) \approx \underline{x}^2$, the x_\perp and y_\perp integrations in Eq. (23) can be done exactly yielding

$$\frac{d\sigma^{pA}}{d^2k \, dy} = \frac{\alpha_s C_F}{\pi^2} \int d^2b \left\{ -\frac{1}{\underline{k}^2} + \frac{2}{\underline{k}^2} e^{-\underline{k}^2/Q_{s0}^2} + \frac{1}{Q_{s0}^2} e^{-\underline{k}^2/Q_{s0}^2} \left[\ln \frac{Q_{s0}^4}{4 \Lambda^2 \underline{k}^2} + \text{Ei} \left(\frac{\underline{k}^2}{Q_{s0}^2} \right) \right] \right\}, \quad (24)$$

where $\text{Ei}(x)$ is the exponential integral. Our goal is to construct the ratio of the number of gluons produced in a pA collision over the number of gluons produced in a pp collision scaled by the number of collisions

$$R^{pA}(\underline{k}, y) = \frac{\frac{d\sigma^{pA}}{d^2k \, dy}}{A \frac{d\sigma^{pp}}{d^2k \, dy}}. \quad (25)$$

In the same approximation in which Eq. (24) is derived the gluon production cross section in pp scaled up by A is given by

$$A \frac{d\sigma^{pp}}{d^2k \, dy} = \frac{\alpha_s C_F}{\pi^2} \int_A d^2b \frac{Q_{s0}^2}{\underline{k}^4}, \quad (26)$$

which can be obtained for instance by taking the $k_T/Q_{s0} \gg 1$ limit of Eq. (24) and using the fact that $Q_{s0}^2 \sim A^{1/3}$. For a cylindrical nucleus the impact parameter \underline{b} integration would just give a factor of S_A . Using Eqs. (24) and (26) in Eq. (25) we then obtain

$$R^{pA}(k_T) = \frac{\underline{k}^4}{Q_{s0}^2} \left\{ -\frac{1}{\underline{k}^2} + \frac{2}{\underline{k}^2} e^{-\underline{k}^2/Q_{s0}^2} + \frac{1}{Q_{s0}^2} e^{-\underline{k}^2/Q_{s0}^2} \left[\ln \frac{Q_{s0}^4}{4 \Lambda^2 \underline{k}^2} + \text{Ei} \left(\frac{\underline{k}^2}{Q_{s0}^2} \right) \right] \right\}. \quad (27)$$

The ratio $R^{pA}(k_T)$ is plotted in Fig. 4 for $\Lambda = 0.2 Q_{s0}$. It clearly exhibits an enhancement at high- k_T typical of Cronin effect [44]. Similar conclusions regarding formula (23) have been reached earlier in [45,46].

It is worth noting that expanding $R^{pA}(k)$ from Eq. (27) in the powers of Q_{s0}/k_T (“twists”) yields a series with only positive terms

$$R^{pA}(k_T) = 1 + 2 \frac{Q_{s0}^2}{\underline{k}^2} + 6 \frac{Q_{s0}^4}{\underline{k}^4} + 24 \frac{Q_{s0}^6}{\underline{k}^6} + \dots = \sum_{n=0}^{\infty} n! \left(\frac{Q_{s0}^2}{\underline{k}^2} \right)^n. \quad (28)$$

The series (28) is divergent, but it is Borel resummable with the sum given by Eq. (27), though not all terms in Eq. (27) can be reconstructed by Borel resummation procedure.

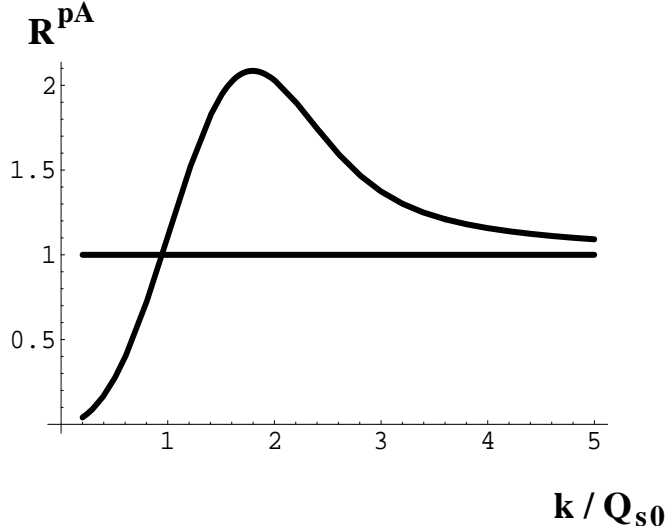


FIG. 4. The ratio R^{pA} for gluons plotted as a function of k_T/Q_{s0} in the quasi-classical McLerran-Venugopalan model as found in [26].

To establish whether inclusion of the correct transverse size dependence in the exponents of Eq. (23) would change the conclusion about Cronin effect let us study the high- k_T asymptotic of Eq. (23). A simple calculation yields

$$\begin{aligned} \frac{d\sigma^{pA}}{d^2k dy} &= \frac{\alpha_s C_F}{\pi^2} \int d^2b \frac{Q_{s0}^2}{\underline{k}^4} \left[\left(\ln \frac{\underline{k}^2}{4\Lambda^2} + 2\gamma - 1 \right) + \right. \\ &+ \left. \frac{Q_{s0}^2}{4\underline{k}^2} \left(6 \ln^2 \frac{\underline{k}^2}{4\Lambda^2} - 8(4-3\gamma) \ln \frac{\underline{k}^2}{4\Lambda^2} + 29 + 24\gamma^2 - 64\gamma \right) + \dots \right], \quad k_T \rightarrow \infty. \end{aligned} \quad (29)$$

For a cylindrical nucleus, keeping only the leading logarithmic ($\ln \frac{\underline{k}^2}{\Lambda^2}$) terms in the parentheses of Eq. (29) we obtain

$$R^{pA}(k_T) = 1 + \frac{3}{2} \frac{Q_{s0}^2}{\underline{k}^2} \ln \frac{\underline{k}^2}{\Lambda^2} + \dots, \quad k_T \rightarrow \infty \quad (30)$$

indicating that R^{pA} approaches 1 from above at high k_T , which is typical of Cronin enhancement. We therefore conclude that in the framework of the quasi-classical approximation employed in [26] the ratio R^{pA} is less than 1 at small $k_T \lesssim Q_{s0}$ and has Cronin enhancement at high $k_T \gtrsim Q_{s0}$.

B. Sum Rule

Let us now prove a sum rule for gluon production cross section in pA collisions similar to the sum rule which we proved for gluon distributions in Sect. II B. First we have to rewrite Eq. (23) in a k_T -factorized form [8,40,39]. Of course it is not obvious *a priori* that Eq. (23) can be rewritten in a k_T -factorized form. Repeating the steps outlined in Sect. IV of [39] we first perform one of the transverse coordinate integrations in Eq. (23) rewriting it as

$$\frac{d\sigma^{pA}}{d^2k dy} = \frac{1}{2\pi^2} \frac{\alpha_s C_F}{\pi} \int d^2b d^2z e^{-i\underline{k}\cdot\underline{z}} \left[2i \frac{\underline{z} \cdot \underline{k}}{\underline{z}^2 \underline{k}^2} - \ln \frac{1}{z_T \Lambda} \right] N_G(\underline{z}, \underline{b}, 0), \quad (31)$$

where $N_G(\underline{z}, \underline{b}, 0)$ is given by Eq. (9). Using the fact that $N_G(z=0, \underline{b}, 0) = 0$ we write Eq. (31) as

$$\frac{d\sigma^{pA}}{d^2k dy} = \frac{1}{2\pi^2} \frac{\alpha_s C_F}{\pi} \frac{1}{\underline{k}^2} \int d^2b d^2z N_G(\underline{z}, \underline{b}, 0) \nabla_z^2 \left(e^{-i\underline{k}\cdot\underline{z}} \ln \frac{1}{z_T \Lambda} \right). \quad (32)$$

Let us denote the forward scattering amplitude of a gluon dipole of transverse size \underline{r} on a single nucleon (proton) integrated over the impact parameter \underline{b}' of the dipole measured with respect to the proton by

$$\int d^2b' n_G(\underline{r}, \underline{b}', y=0) = \pi \alpha_s^2 \underline{r}^2 \ln \frac{1}{r_T \Lambda}. \quad (33)$$

Eq. (33) is obtained by expanding Eq. (9) at the leading order and taking $A = 1$. It corresponds to the two gluon exchange interaction between the dipole and the proton. In the quasi-classical Glauber-Mueller approximation in which Eq. (9) is derived each nucleon exchanges only two gluons with the dipole [43,12]. Therefore Eq. (33) is a natural reduction of Eq. (9) to a single nucleon case.

With the help of Eq. (33) we rewrite Eq. (32) as [39]

$$\frac{d\sigma^{pA}}{d^2k dy} = \frac{C_F}{\alpha_s \pi (2\pi)^3} \frac{1}{\underline{k}^2} \int d^2B d^2b d^2z \nabla_z^2 n_G(\underline{z}, \underline{b} - \underline{B}, 0) e^{-i\underline{k}\cdot\underline{z}} \nabla_z^2 N_G(\underline{z}, \underline{b}, 0). \quad (34)$$

Now \underline{B} is the impact parameter of the proton with respect to the center of the nucleus and \underline{b} is the impact parameter of the gluon with respect to the center of the nucleus as shown in Fig. 5.

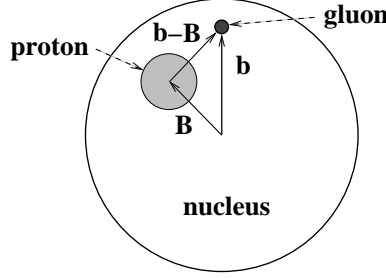


FIG. 5. Gluon production in pA collisions as seen in the transverse plane. To make the picture easier to read the gluon is placed far away from the proton which is highly unlikely to happen in real life.

Eq. (34) is the expression for gluon production one would write in the k_T -factorization approach [40]. To see this explicitly let us rewrite Eq. (34) in terms of the unintegrated gluon distribution function from Eq. (2). One easily derives

$$\frac{d\sigma^{pA}}{d^2k dy} = \frac{2\alpha_s}{C_F} \frac{1}{k^2} \int d^2q \phi_p(\underline{q}) \phi_A(\underline{k} - \underline{q}), \quad (35)$$

which is the same formula as obtained in k_T -factorization approach [8,47,40]. ϕ_p is defined as unintegrated gluon distribution of the proton given by Eq. (2) with n_G instead of N_G on the right hand side. Eq. (35) demonstrates that the gluon production cross section in pA can be expressed in terms of the gluon distribution (2) in a rather straightforward way [39]. Somehow it is the distribution (2) and not the Weizsäcker-Williams distribution (6) that enters Eq. (35).

Eq. (35) demonstrates that, at least in the framework of McLerran-Venugopalan model, the multiple rescattering leading to Cronin enhancement in pA can be incorporated in the gluon distribution functions [26,30]. There is no clear distinction between the nuclear wave function effects and the Glauber-type rescatterings in the nucleus. Anti-shadowing present in the gluon distribution function $\phi_A(\underline{k})$ as shown in Fig. 3 simply translates into Cronin effect of Fig. 4 via Eq. (35).

To prove the sum rule we note that Eq. (34) implies that

$$\int d^2k \frac{d\sigma^{pA}}{d^2k dy} = \frac{C_F}{\alpha_s 2\pi^2} \int d^2B d^2b [\nabla_z^2 n_G(\underline{z}, \underline{b} - \underline{B}, 0)] \Big|_{\underline{z}=0} [\nabla_z^2 N_G(\underline{z}, \underline{b}, 0)] \Big|_{\underline{z}=0}. \quad (36)$$

Since at very small \underline{z} the nonlinear evolution effects of Eq. (41) and multiple rescatterings of Eq. (9) will disappear, similar to Eq. (10) we write

$$[\nabla_z^2 N_G(\underline{z}, \underline{b}, y=0)] \Big|_{\underline{z}=0} = A^{1/3} [\nabla_z^2 n_G(\underline{z}, \underline{b}, y=0)] \Big|_{\underline{z}=0}. \quad (37)$$

The impact parameter integration in pA will give an extra factor of $A^{2/3}$ as compared to pp. Together with Eq. (37) this gives

$$\int d^2k \frac{d\sigma^{pA}}{d^2k dy} = A \int d^2k \frac{d\sigma^{pp}}{d^2k dy}. \quad (38)$$

The sum rule we obtained in Eq. (38) implies that as long as the condition (37) holds the average transverse momentum squared of the gluons produced in pA collisions is equal to $A^{1/3}$ times the same quantity for pp collisions. In McLerran-Venugopalan model the dipole forward scattering amplitude is given by Glauber-Mueller expression (9) for which Eq. (37) is always true and the sum rule (38) holds.

Similar to the sum rule proved in Sect. II for gluon distribution functions, the sum rule (38) insures that if the gluon production cross section in pA collisions is, in some region of k_T , smaller than A times the gluon production cross section in pp than there should be some other region of k_T in which their roles are reversed. For R^{pA} defined in Eq. (25) that means that if, in some region of k_T , it is less than 1 there must be some other region of k_T in which it is greater than 1. Of course the \underline{k}^2 factors in Eq. (38) make the quantitative

amounts of suppression and enhancement very different from the ones dictated by, for instance, the sum rule of Sect. II.

Before we proceed let us illustrate how the sum rule (38) works with a simple example. In the quasi-classical approximation for the gluon production in pA considered above R^{pA} is below 1 at $k_T \lesssim Q_{s0}$. Expanding Eq. (27) for $k_T \ll Q_{s0}$ we write

$$R^{pA}(k) \approx \frac{k^2}{Q_{s0}^2} \ll 1 \quad \text{if} \quad k_T \ll Q_{s0}. \quad (39)$$

Eq. (39), together with the sum rule (38) imply that there must exist a region of k_T with a Cronin-like enhancement of gluon production, which is demonstrated by the full answer plotted in Fig. 4.

Let us note again that the sum rule (38) does not preclude the possibility of high- k_T suppression. In the given example the absence of high- k_T suppression is insured by the fact that in the quasi-classical approximation the cross section (23) depends only on one momentum scale Q_{s0} (Λ -dependence is rather weak). The corresponding R^{pA} (27) can only have one extremum determined by Q_{s0} , which is the Cronin maximum in Fig. 4. Below we will see that the effects of quantum evolution can bring in other momentum scales resulting in a more complicated behavior of R^{pA} .

IV. INCLUDING SMALL- X EVOLUTION: CRONIN EFFECT AND HIGH- P_T SUPPRESSION

A. Including Small- x Evolution

As the energy of the collisions increases quantum evolution corrections become important. For produced particles with the same k_T higher energy implies smaller effective Bjorken x meaning that the quantum corrections of the type $\alpha_s \ln 1/x$ should be resummed. These corrections can be resummed by the BFKL equation [31], which calculates the contribution of the hard (perturbative) pomeron. However, as energy increases multiple pomeron exchanges become important, resulting in a more complicated small- x evolution [36,37]. In [32,35] an equation was constructed which resums multiple pomeron exchanges for a forward amplitude of a $q\bar{q}$ dipole scattering on a nucleus in the large N_c limit. The forward amplitude $N(\underline{r}, \underline{b}, Y)$ of a dipole of transverse size \underline{r} scattering at impact parameter \underline{b} and rapidity Y was normalized such that the total $q\bar{q}A$ cross section was given by

$$\sigma_{tot}^{q\bar{q}A} = 2 \int d^2b N(\underline{r}, \underline{b}, Y). \quad (40)$$

The evolution equation for $N(\underline{r}, \underline{b}, Y)$ closes only in the large- N_c limit of QCD [35,36] and reads [32–34]

$$\begin{aligned} N(\underline{x}_{01}, \underline{b}, Y) &= N(\underline{x}_{01}, \underline{b}, Y=0) e^{-\frac{4\alpha C_F}{\pi} \ln(\frac{\underline{x}_{01}}{\rho}) Y} + \frac{\alpha C_F}{\pi^2} \int_0^Y dy e^{-\frac{4\alpha C_F}{\pi} \ln(\frac{\underline{x}_{01}}{\rho})(Y-y)} \\ &\times \int_\rho d^2x_2 \frac{x_{01}^2}{x_{02}^2 x_{12}^2} [2 N(\underline{x}_{02}, \underline{b} + \frac{1}{2}\underline{x}_{12}, y) - N(\underline{x}_{02}, \underline{b} + \frac{1}{2}\underline{x}_{12}, y) N(\underline{x}_{12}, \underline{b} + \frac{1}{2}\underline{x}_{02}, y)], \end{aligned} \quad (41)$$

with the initial condition given by $N(\underline{x}_{01}, \underline{b}, Y=0)$ taken to be of Mueller-Glauber form [43] in [32]:

$$N(\underline{x}_{01}, \underline{b}_0, Y=0) = 1 - e^{-\underline{x}_{01}^2 Q_{0s}^{\text{quark}2} \ln(1/x_{01T}\Lambda)/4}, \quad (42)$$

where

$$N_c Q_{0s}^{\text{quark}2} = C_F Q_{s0}^2. \quad (43)$$

In [39] it was shown how to resum the effects of nonlinear evolution of Eq. (41) for gluon production in DIS. In the quasi-classical approximation the gluon production in DIS is given by a formula similar to Eq. (23) [41]. That formula can also be recast in a k_T factorized from of Eq. (34) [39]. As was proven in [39]

in order to include quantum evolution (41) in Eq. (34) for DIS one has to make replacements. First, one has to replace $N_G(\underline{z}, \underline{b}, 0)$ in Eq. (34) by the forward quark dipole amplitude using the following expression valid in the large- N_c limit [39]

$$N_G(\underline{z}, \underline{b}, y) = 2N(\underline{z}, \underline{b}, y) - N(\underline{z}, \underline{b}, y)^2, \quad (44)$$

where $N(\underline{z}, \underline{b}, y)$ is the forward scattering amplitude of a $q\bar{q}$ dipole on a nucleus evolved by nonlinear equation (41). Then one has to replace $n_G(\underline{z}, \underline{b}, 0)$ by $n_G(\underline{z}, \underline{b}, Y - y)$ evolved just by the linear part of Eq. (41) (the BFKL equation [31]). Here Y is the total rapidity interval between the projectile (virtual photon) and target nucleus in a DIS collision. The initial conditions for both N_G and n_G evolution are given by $N_G(\underline{z}, \underline{b}, 0)$ and $n_G(\underline{z}, \underline{b}, 0)$ correspondingly.

Since both pA and DIS are considered here as scatterings of an unsaturated projectile (proton or $q\bar{q}$ pair) on a saturated target (nucleus) with the gluon production in the quasi-classical limit given by the same Eq. (34), we may conjecture that inclusion of quantum evolution (41) in gluon production cross section is done similarly for both processes. We therefore write

$$\frac{d\sigma^{pA}}{d^2k dy} = \frac{C_F}{\alpha_s \pi (2\pi)^3} \frac{1}{\underline{k}^2} \int d^2B d^2b d^2z \nabla_z^2 n_G(\underline{z}, \underline{b} - \underline{B}, Y - y) e^{-i\underline{k}\cdot\underline{z}} \nabla_z^2 N_G(\underline{z}, \underline{b}, y), \quad (45)$$

where Y is the total rapidity interval between the proton and the nucleus. Just like in DIS N_G in Eq. (45) is given by Eq. (44), where N should be found from Eq. (41), while n_G should be determined from the linear part of Eq. (45) (BFKL) with the initial conditions given by Eq. (33). Eq. (45) is exact if the proton is modeled as a diquark–quark pair [52], in which case it would be identical to $q\bar{q}$ pair produced by a virtual photon in DIS. In general case Eq. (45) remains a well-motivated conjecture.

Since the inclusion of quantum evolution yielded us Eq. (45) which is identical in structure to Eq. (34), the sum rule of Eq. (38) also holds for the gluon production cross section of Eq. (45) as long as the condition (37) is satisfied by the evolved N_G :

$$[\nabla_z^2 N_G(\underline{z}, \underline{b}, y)] \Big|_{\underline{z}=0} = A^{1/3} [\nabla_z^2 n_G(\underline{z}, \underline{b}, y)] \Big|_{\underline{z}=0}. \quad (46)$$

Therefore, since the gluon production spectrum in pA given by Eq. (45) exhibits saturation features at small k_T leading to $R^{pA} < 1$ it is bound to have Cronin effect at higher k_T . The important question we want to address here is whether the ratio R^{pA} remains greater than 1 for large k_T to the right of Cronin maximum as shown in Fig. 4, or the effect of quantum evolution would be to modify the high- k_T asymptotic introducing suppression of the produced gluons as was suggested in [7].

In the following we are going to study effects of evolution equation (41) on the gluon spectrum and on R^{pA} at high k_T . Our goal is to determine whether R^{pA} is approaching 1 at high k_T from above or from below. The latter case would correspond to high- k_T suppression. To simplify the discussion we will consider a cylindrical nucleus for which Eq. (45) reduces to

$$\frac{d\sigma^{pA}}{d^2k dy} = \frac{C_F}{\alpha_s \pi (2\pi)^3} \frac{S_p S_A}{\underline{k}^2} \int d^2z \nabla_z^2 n_G(\underline{z}, Y - y) e^{-i\underline{k}\cdot\underline{z}} \nabla_z^2 N_G(\underline{z}, y), \quad (47)$$

with S_p the cross sectional area of the proton.

B. Leading Twist Effects

1. Leading Twist Gluon Production Cross Section

We start by exploring the leading high- k_T behavior of the gluon spectrum given by Eq. (47). At very high k_T the integral in Eq. (47) is dominated by small values of z_T . Therefore we can neglect the quadratic term in the evolution equation for N_G (41) leaving only the linear part – the BFKL evolution with initial conditions for a gluon dipole given by Eq. (9). The corresponding Feynman diagram is shown in Fig. 6. The solution of the BFKL equation is well-known and reads

$$N_{G1}(\underline{z}, y) = \int \frac{d\lambda}{2\pi i} C_\lambda^A (z_T Q_{s0})^\lambda e^{2\bar{\alpha}_s \chi(\lambda) y} \quad (48)$$

with

$$\bar{\alpha}_s = \frac{\alpha_s N_c}{\pi}, \quad (49)$$

$$\chi(\lambda) = \psi(1) - \frac{1}{2} \psi\left(1 - \frac{\lambda}{2}\right) - \frac{1}{2} \psi\left(\frac{\lambda}{2}\right) \quad (50)$$

and Q_{s0} for a cylindrical nucleus given by Eq. (18). The coefficient C_λ^A is fixed from the initial conditions at $y = 0$ given by Eq. (9). Then for small $z_T < 1/Q_{s0}$

$$\begin{aligned} C_\lambda^A &= \sum_{n=1}^{\infty} \sum_{m=0}^n \frac{(-1)^{n+1}}{4^n (n-m)! (2n-\lambda)^{m+1}} \ln^{n-m} \frac{Q_{s0}}{\Lambda} \\ &= \sum_{n=1}^{\infty} \frac{1}{4^n n! (\lambda - 2n)^{n+1}} \left(\frac{Q_{s0}}{\Lambda}\right)^{2n-\lambda} \Gamma\left(1+n, (2n-\lambda) \ln \frac{Q_{s0}}{\Lambda}\right). \end{aligned} \quad (51)$$

Similarly for the gluon dipole cross section on the proton we write

$$n_G(\underline{z}, y) = \int \frac{d\lambda}{2\pi i} C_\lambda^p (z_T \Lambda)^\lambda e^{2\bar{\alpha}_s \chi(\lambda) y}, \quad (52)$$

where now the scale characterizing the proton is given by

$$\Lambda^2 = 4\pi \alpha_s^2 \frac{1}{S_p}. \quad (53)$$

The coefficient C_λ^p is obtained by requiring that Eq. (52) reduces to Eq. (33) when $y = 0$. For $z_T < 1/\Lambda$ we derive

$$C_\lambda^p = \frac{1}{4(\lambda-2)^2}. \quad (54)$$

(We have identified the non-perturbative scale characterizing the proton (53) with the infrared cutoff employed earlier in Eq. (33).)

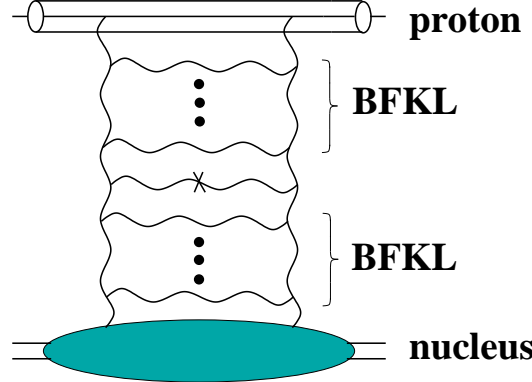


FIG. 6. Gluon production in pA collisions at the leading twist level (see text).

Substituting Eqs. (48) and (52) into Eq. (47) and integrating over z yields [53,54]

$$\begin{aligned} \frac{d\sigma^{pA}}{d^2k dy} \Big|_{LT} &= \frac{C_F S_p S_A}{4 \alpha_s (2\pi)^3} \int \frac{d\lambda}{2\pi i} \frac{d\lambda'}{2\pi i} \lambda^2 \lambda'^2 C_\lambda^A C_{\lambda'}^p 2^{\lambda+\lambda'} \frac{\Gamma\left(-1 + \frac{\lambda+\lambda'}{2}\right)}{\Gamma\left(2 - \frac{\lambda+\lambda'}{2}\right)} \left(\frac{Q_{s0}}{k_T}\right)^\lambda \left(\frac{\Lambda}{k_T}\right)^{\lambda'} \\ &\times e^{2\bar{\alpha}_s [\chi(\lambda) y + \chi(\lambda') (Y-y)]}. \end{aligned} \quad (55)$$

Eq. (55) gives the leading twist expression for the gluon production cross section in pA collisions and is illustrated in Fig. 6.

The difference between Eq. (55) and Eq. (13) of [53] is in gamma-functions in the integrand. The difference manifests itself at the order of higher twists, where the gluon distributions used in [53], if taken at $y = 0$ and used in inverted Eq. (2) to obtain n_p , would yield higher twist corrections (higher powers of r_T) to the right hand side of Eq. (33), which should not be there in the two-gluon exchange approximation corresponding to $y = 0$ limit.

2. Double Logarithmic Approximation: Monojet Versus Dijet and First Signs of High- p_T Suppression

To derive the high- k_T behavior of the gluon production cross section in Eq. (55) we have to evaluate the integrals in it by saddle point method. When $k_T \gg Q_{s0}, \Lambda$ we approximately write

$$\chi(\lambda) \approx \frac{1}{2 - \lambda}. \quad (56)$$

Then the saddle points are given by

$$\lambda_{sp} = 2 - \sqrt{\frac{2\bar{\alpha}_s y}{\ln(k_T/Q_{s0})}} \quad (57)$$

and

$$\lambda'_{sp} = 2 - \sqrt{\frac{2\bar{\alpha}_s (Y-y)}{\ln(k_T/\Lambda)}}. \quad (58)$$

Integrating over λ and λ' around the saddle points (57) and (58) in Eq. (55) yields gluon production cross section in double logarithmic approximation (DLA) [47]

$$\begin{aligned} \frac{d\sigma^{pA}}{d^2k dy} \Big|_{DLA} &\approx \frac{C_F S_p S_A}{\alpha_s (2\pi)^4} \frac{Q_{s0}^2 \Lambda^2}{\underline{k}^4} \frac{1}{2\bar{\alpha}_s} \left[\frac{\ln \frac{k_T}{Q_{s0}} \ln \frac{k_T}{\Lambda}}{y^3 (Y-y)^3} \right]^{1/4} \left(\sqrt{\frac{y}{\ln \frac{k_T}{Q_{s0}}}} + \sqrt{\frac{Y-y}{\ln \frac{k_T}{\Lambda}}} \right) \\ &\times \exp \left(2\sqrt{2\bar{\alpha}_s y \ln \frac{k_T}{Q_{s0}}} + 2\sqrt{2\bar{\alpha}_s (Y-y) \ln \frac{k_T}{\Lambda}} \right). \end{aligned} \quad (59)$$

To understand Eq. (59) let us first construct gluon distribution function

$$xG_A(x, Q^2) = \int_{\Lambda^2}^{Q^2} dk_T^2 \phi^A(x, \underline{k}^2) \quad (60)$$

in the same double logarithmic approximation [9]. Using Eq. (48) in Eqs. (2) and (60) we obtain in the double logarithmic approximation

$$xG_A(x, Q^2) = \frac{C_F S_A Q_{s0}^2}{\alpha_s (2\pi)^3} 2\sqrt{\pi} \frac{\ln^{1/4} \frac{Q}{Q_{s0}}}{(2\bar{\alpha}_s \ln(1/x))^{3/4}} e^{2\sqrt{2\bar{\alpha}_s \ln(1/x) \ln(Q/Q_{s0})}}. \quad (61)$$

Since the above gluon distribution is obtained in the DLA (large Q^2) limit of the BFKL equation, it can also be obtained by taking the small- x limit of the DGLAP equation [55]. One can explicitly check that with the help of Eq. (61) and an analogous one for the proton gluon distribution xG_p , Eq. (59) can be rewritten as

$$\begin{aligned} \frac{d\sigma^{pA}}{d^2k dy} = & \frac{2\alpha_s}{C_F \underline{k}^2} \left[xG_p(x = e^{-Y+y}, \underline{k}^2) \frac{\partial}{\partial k_T^2} xG_A(x = e^{-y}, \underline{k}^2) + \right. \\ & \left. + xG_A(x = e^{-y}, \underline{k}^2) \frac{\partial}{\partial k_T^2} xG_p(x = e^{-Y+y}, \underline{k}^2) \right]. \end{aligned} \quad (62)$$

Eq. (62) can be obtained directly by using Eq. (61) in Eq. (35) and assuming that the q -integration in Eq. (35) is dominated by the regions near $\underline{q} = 0$ and $\underline{q} = \underline{k}$ [8,47]. As was shown in detail in [10], Eq. (62) can be reduced to

$$\begin{aligned} \frac{d\sigma^{pA}}{d^2k dy} = & \frac{2}{\pi N_c C_F} \left(\int_{e^{-Y+y}}^1 \frac{dx_1}{x_1} x_1 G_p(x_1, \underline{k}^2) xG_A(x = e^{-y}, \underline{k}^2) + \right. \\ & \left. + \int_{e^{-y}}^1 \frac{dx_1}{x_1} xG_p(x = e^{-Y+y}, \underline{k}^2) x_1 G_A(x_1, \underline{k}^2) \right) \frac{d\hat{\sigma}^{gg \rightarrow gg}}{d^2k}, \end{aligned} \quad (63)$$

which is the standard dijet production cross section derived in collinear factorization approximation (see e.g. [10]). (Of course one of the jets' momentum in Eq. (63) is integrated over.) Therefore, we have started with a single jet production cross section given by k_T -factorized expression (55) with BFKL gluon distributions and demonstrated that in the large k_T limit it reduces to the conventional dijet production cross section (63) given by collinear factorization with DGLAP-evolved structure functions.¹

Before we continue let us study R^{pA} given by the cross section of Eq. (59). The naive expectation for the high- k_T limit of the leading twist gluon production cross section would be that $R^{pA} = 1$. However, already at the level of approximation employed in Eq. (59) this is not quite the case. To see this let us first write down an expression for the gluon production cross section in pp collisions in the leading twist DLA approximation. It is obtained by replacing Q_{s0} and S_A in Eq. (59) by Λ and S_p correspondingly. We obtain

$$\frac{d\sigma^{pp}}{d^2k dy} \Big|_{DLA} \approx \frac{C_F S_p^2}{\alpha_s (2\pi)^4} \frac{\Lambda^4}{\underline{k}^4} \frac{1}{2\bar{\alpha}_s} \frac{\sqrt{y} + \sqrt{Y-y}}{y^{3/4} (Y-y)^{3/4}} \exp \left[2\sqrt{2\bar{\alpha}_s \ln \frac{k_T}{\Lambda}} (\sqrt{y} + \sqrt{Y-y}) \right]. \quad (64)$$

To calculate R^{pA} we note that since $S_A = A^{2/3} S_p$ one concludes from Eqs. (18) and (53) that $Q_{s0}^2 = A^{1/3} \Lambda^2$. Using Eqs. (59) and (64) in Eq. (25) yields

$$\begin{aligned} R^{pA}(k_T, y) \Big|_{k_T \gg Q_s} = & \frac{\left(\ln \frac{k_T}{Q_{s0}} \ln \frac{k_T}{\Lambda} \right)^{1/4}}{\sqrt{y} + \sqrt{Y-y}} \left(\sqrt{\frac{y}{\ln \frac{k_T}{Q_{s0}}}} + \sqrt{\frac{Y-y}{\ln \frac{k_T}{\Lambda}}} \right) \\ & \times \exp \left[2\sqrt{2\bar{\alpha}_s y} \left(\sqrt{\ln \frac{k_T}{Q_{s0}}} - \sqrt{\ln \frac{k_T}{\Lambda}} \right) \right], \end{aligned} \quad (65)$$

where $Q_s = Q_s(y)$ is the full energy dependent saturation scale, which reduces to Q_{s0} at $y = 0$. Defining

$$\xi \equiv \left(\frac{\ln \frac{k_T}{Q_{s0}}}{\ln \frac{k_T}{\Lambda}} \right)^{1/4} \quad (66)$$

¹We thank Al Mueller for encouraging one of the authors (Yu. K.) to verify this correspondence explicitly several years ago.

we rewrite Eq. (65) as

$$R^{pA}(\xi, y) \Big|_{\xi < 1} = \frac{\frac{1}{\xi} \sqrt{y} + \xi \sqrt{Y-y}}{\sqrt{y} + \sqrt{Y-y}} \exp \left[-2 \sqrt{2 \bar{\alpha}_s y \frac{1-\xi^2}{1+\xi^2} \ln \frac{Q_{s0}}{\Lambda}} \right] \quad (67)$$

where $\xi < 1$ for $k_T > Q_{s0}$, since $Q_{s0}^2 = A^{1/3} \Lambda^2 \gg \Lambda^2$. For large transverse momenta in question, $k_T \gg Q_s(y)$, the variable ξ is approaching 1 from below as is clear from Eq. (66). In the limit $\xi \rightarrow 1$ Eq. (67) becomes

$$R^{pA}(\xi, y) \Big|_{\xi \rightarrow 1} \approx \left(1 + (1-\xi) \frac{\sqrt{y} - \sqrt{Y-y}}{\sqrt{y} + \sqrt{Y-y}} \right) \exp \left[-2 \sqrt{2 \bar{\alpha}_s y (1-\xi) \ln \frac{Q_{s0}}{\Lambda}} \right]$$

$$< (2-\xi) \exp \left[-2 \sqrt{2 \bar{\alpha}_s y (1-\xi) \ln \frac{Q_{s0}}{\Lambda}} \right] \approx \exp \left[-2 \sqrt{2 \bar{\alpha}_s y (1-\xi) \ln \frac{Q_{s0}}{\Lambda}} \right] < 1, \quad k_T \gg Q_s(y). \quad (68)$$

We neglected $2-\xi = 1+(1-\xi)$ in front of the exponent in Eq. (68) since the $(1-\xi)$ correction to 1 in it is not enhanced by any parametrically large variables, such as y and $\ln Q_{s0}/\Lambda$ in the exponent. If $R^{pA}(\xi, y)$ from Eq. (68) is expanded in powers of $(1-\xi)$ this prefactor term would give subleading logarithmic corrections to the expansion of the exponent, which are negligible in the DLA limit considered here.

We conclude that R^{pA} from Eq. (65) is smaller than one. Since $R^{pA}(\xi, y)$ in Eq. (68) is an increasing function of ξ and ξ is an increasing function of k_T , we observe that $R^{pA}(k_T, y)$ in Eq. (65) is an increasing function of k_T approaching 1 from below. This suppression is mainly due to the difference of the cutoffs in the logarithms of transverse momentum in the exponent of Eq. (65). The cutoff for the nucleus case is given by nuclear saturation scale, which is different from the appropriate scale in a single proton. The high momentum regions, where linear evolution equations work, are cut off from below by saturation scales, which are different for different nuclei and for the proton. In this way, as we can see from Eqs. (65) and (68), saturation influences the physics at high k_T as long as corresponding x_{Bj} is small. The effect of saturation is to introduce high- k_T suppression.

Let us emphasize here that the suppression of Eq. (68) does not rule out Cronin effect discussed below. Instead, due to the sum rule of Eq. (38), it demands existence of Cronin enhancement.

The suppression of Eq. (68) is a leading twist effect and is due to quantum evolution. In this sense it is similar to the suppression suggested in [7]. However, the suppression of [7] corresponds to a region of lower k_T , where the double logarithmic approximation of Eq. (65) is not valid any more. There the suppression happens due to the change in anomalous dimension of the gluon distribution function, as we are going to discuss below.

3. Onset of Anomalous Dimension: More High- p_T Suppression

For the values of k_T lower than considered above (but still much larger than Q_{s0}) the saddle point of λ -integration in Eq. (55) shifts to a smaller value than given by Eq. (57). While in determining the saddle point of Eq. (57) we had to expand $\chi(\lambda)$ around $\lambda = 2$, now we have to expand it around $\lambda = 1$. There one writes

$$\chi(\lambda) \approx 2 \ln 2 + \frac{7}{4} \zeta(3) (\lambda - 1)^2 \quad (69)$$

obtaining the value of the saddle point

$$\lambda_{sp}^* = 1 + \frac{\ln \frac{k_T}{Q_{s0}}}{7 \zeta(3) \bar{\alpha}_s y}. \quad (70)$$

As was suggested in [42], the transition of the saddle point from the value given in Eq. (57) to the one given in Eq. (70) happens around

$$k_{\text{geom}} \approx Q_s(y) \frac{Q_s(y)}{Q_{s0}} \quad (71)$$

indicating the onset of geometric scaling regime [48]. Here in the double logarithmic approximation the saturation scale depends on energy as [49,42]

$$Q_s(y) \approx Q_{s0} e^{2\bar{\alpha}_s y}. \quad (72)$$

The precise value of the scale k_{geom} in Eq. (71) depends on the definition of the saturation scale and on the way one defines the transition between the double logarithmic and geometric scaling regions. For instance, if we define the transition by equating the saddle points of Eqs. (57) and (70)

$$\lambda_{sp} = \lambda_{sp}^*, \quad (73)$$

we get at the point of closest approach (the two saddle point values are never equal to each other)

$$k_{\text{geom}} = Q_{s0} e^{\bar{\alpha}_s y} 7^{2/3} \zeta(3)^{2/3} 2^{-1/3} \approx Q_{s0} e^{3.28 \bar{\alpha}_s y}. \quad (74)$$

When combined with the saturation scale from Eq. (72) this gives

$$k_{\text{geom}} \approx Q_s(y) \left(\frac{Q_s(y)}{Q_{s0}} \right)^{0.64}, \quad (75)$$

which is slightly different from Eq. (71). At the same time, using the energy dependence of the saturation scale found in [56] in the fixed coupling case

$$Q_s(y) \approx Q_{s0} e^{2.44 \bar{\alpha}_s y} \quad (76)$$

in Eq. (74) gives

$$k_{\text{geom}} \approx Q_s(y) \left(\frac{Q_s(y)}{Q_{s0}} \right)^{0.34}, \quad (77)$$

which is even lower than Eq. (75). A definition of the transition point different from Eq. (73) would give slightly different estimates for k_{geom} .

Nevertheless, the ambiguities in the scale k_{geom} notwithstanding, one can argue, as was done in [42], that there exists a large momentum scale k_{geom} , which is parametrically larger than the saturation scale

$$k_{\text{geom}} \gg Q_s(y). \quad (78)$$

For $k_T \gtrsim k_{\text{geom}}$ there is no geometric scaling and the gluon production is well described by double logarithmic approximation described above resulting in R^{pA} from Eq. (65). $k_T \lesssim k_{\text{geom}}$ is the region of geometric scaling [42]. When $k_T \lesssim Q_s(y)$ (saturation region) multiple pomeron exchanges become important leading to the saturation of structure functions [8]. For $Q_s(y) \lesssim k_T \lesssim k_{\text{geom}}$ (extended geometric scaling region) multiple pomeron exchanges are not important yet and the gluon production cross section is described by the leading twist expression in Eq. (55) with the λ -integral evaluated near the saddle point of Eq. (70) [7].

Performing the λ and λ' integrals in Eq. (55) in the saddle point approximation around the saddle points of Eqs. (70) and (58) correspondingly yields

$$\begin{aligned} \left. \frac{d\sigma^{pA(1)}}{d^2 k \, dy} \right|_{LLA} &\approx \frac{C_F S_p S_A}{\alpha_s (2\pi)^4} \frac{Q_{s0} \Lambda^2}{\underline{k}^3} \frac{C_1^A}{\sqrt{7\zeta(3)}} \frac{\ln^{1/4} \frac{k_T}{\Lambda}}{\bar{\alpha}_s (Y-y)^{3/4} (2\bar{\alpha}_s)^{1/4}} \\ &\times \exp \left[(\alpha_P - 1) y + 2 \sqrt{2\bar{\alpha}_s (Y-y) \ln \frac{k_T}{\Lambda}} - \frac{\ln^2 \frac{k_T}{Q_{s0}}}{14\zeta(3)\bar{\alpha}_s y} \right], \end{aligned} \quad (79)$$

where

$$\alpha_P - 1 = 2\bar{\alpha}_s \ln 2 \quad (80)$$

is the BFKL pomeron intercept [31] and C_1^A is well-approximated by the first term in the series of Eq. (51) for all physically reasonable values of A

$$C_1^A \approx \frac{1}{4} \left(1 + \ln \frac{Q_{s0}}{\Lambda} \right) = \frac{1}{4} \left(1 + \frac{1}{6} \ln A \right). \quad (81)$$

The superscript ⁽¹⁾ in Eq. (79) denotes the leading twist contribution. We assume that in the transverse momentum region where Eq. (79) is valid, $Q_s(y) \lesssim k_T \lesssim k_{\text{geom}}$, the gluon production cross section in pp collisions is still given by Eq. (64). This is a good approximation since if $k_T \gtrsim Q_s(y) \gg \Lambda$ the double logarithmic approximation of Eq. (64) should work. Using Eqs. (79) and (64) in Eq. (25) we obtain

$$\begin{aligned} R^{pA}(k_T, y) \Big|_{Q_s(y) \lesssim k_T \lesssim k_{\text{geom}}} &= \frac{k_T}{Q_{s0}} \frac{2 C_1^A}{\sqrt{7 \zeta(3)}} \frac{\ln^{1/4} \frac{k_T}{\Lambda}}{(2 \bar{\alpha}_s)^{1/4}} \frac{y^{1/4}}{\sqrt{y} + \sqrt{Y - y}} \\ &\times \exp \left[(\alpha_P - 1) y - 2 \sqrt{2 \bar{\alpha}_s y \ln \frac{k_T}{\Lambda}} - \frac{\ln^2 \frac{k_T}{Q_{s0}}}{14 \zeta(3) \bar{\alpha}_s y} \right]. \end{aligned} \quad (82)$$

To determine whether $R^{pA}(k_T, y)$ in Eq. (82) is greater or less than 1 we first drop the slowly varying and constant prefactors in front of the exponent and write

$$R^{pA}(k_T, y) \Big|_{Q_s(y) \lesssim k_T \lesssim k_{\text{geom}}} \sim \frac{k_T}{Q_{s0}} \exp \left[(\alpha_P - 1) y - 2 \sqrt{2 \bar{\alpha}_s y \ln \frac{k_T}{\Lambda}} - \frac{\ln^2 \frac{k_T}{Q_{s0}}}{14 \zeta(3) \bar{\alpha}_s y} \right] \quad (83)$$

keeping only parametrically important factors. To estimate the value of R^{pA} in Eq. (83) in the extended geometric scaling region $Q_s(y) \lesssim k_T \lesssim k_{\text{geom}}$ we substitute $k_T = k_{\text{geom}}$ into Eq. (83) with k_{geom} from Eq. (71). The result yields an asymptotically small value

$$R^{pA}(k_T, y) \Big|_{Q_s(y) \lesssim k_T \lesssim k_{\text{geom}}} \sim e^{-1.65 \bar{\alpha}_s y} \ll 1, \quad (84)$$

where we used $A = 197$ for gold nucleus. For other values of A and for other values of k_T in the region $Q_s(y) \lesssim k_T \lesssim k_{\text{geom}}$ one still gets exponential suppression for $R^{pA}(k_T, y)$. Therefore we conclude that $R^{pA}(k_T, y) < 1$ in the extended geometric scaling region $Q_s(y) \lesssim k_T \lesssim k_{\text{geom}}$.

As can be checked explicitly, for sufficiently large nucleus (large A), $R^{pA}(k_T, y)$ of Eq. (82) is an increasing function of k for $Q_s(y) \lesssim k_T \lesssim k_{\text{geom}}$. As k_T increases it should smoothly map onto $R^{pA}(k_T, y)$ of Eq. (65), which would approach 1 from below for asymptotically high k_T .

To conclude our discussion of high- k_T suppression at the leading twist level we note that, as was recently argued in [57], the running coupling effects in the BFKL evolution may modify the A -dependence of the saturation scale given by Eqs. (72) and (76), making $Q_s(y)$ almost independent of A at very high energy corresponding to large rapidity y . This would result in high- k_T suppression which would not disappear at any k_T within the extended scaling region. That is $R^{pA}(k_T, y)$ would not approach 1 anymore at high k_T . Instead one would have $R^{pA}(k_T, y) \sim A^{-1/3}$ at high- k_T . This behavior would not contradict the sum rule of Eq. (38), since in this case the condition (46) would not be satisfied any more invalidating the sum rule itself.²

²The argument presented in this paragraph is due to Larry McLerran.

C. Higher Twists

Above we have shown that the effect of quantum evolution (41) on the gluon production cross section in pA with $k_T \gtrsim Q_s(y)$ is to introduce suppression in R^{pA} . Here we would like to study the effect of evolution on the gluon production with $k_T \sim Q_s(y)$, i.e., on the gluons produced at the border of the saturation region. In the fixed coupling case considered throughout the paper the sum rule (38) is valid. As we have demonstrated above, $R^{pA} < 1$ deep inside of the saturation region $k_T \ll Q_s(y)$ (see Eq. (39) for the no-evolution case). The conclusion is also true with quantum evolution (41) included, since the saturation effects still soften the low- k_T gluon spectra in pA compared to pp (see [39,40]). We have just shown that $R^{pA} < 1$ in the region of $k_T > Q_s(y)$. Therefore the sum rule (38) requires Cronin enhancement in the remaining region of $k_T \lesssim Q_s(y)$. This enhancement was indeed observed for the quasi-classical case in Sect. III (see Fig. 4). In fact, inclusion of the next-to-leading twist term already introduced enhancement in that case as can be seen from Eq. (30). Here we are going to show that if one includes the evolution of Eq. (41) into the next-to-leading twist correction to Eq. (55) it would give suppression of R^{pA} at high k_T and would start contributing toward enhancement at lower k_T .

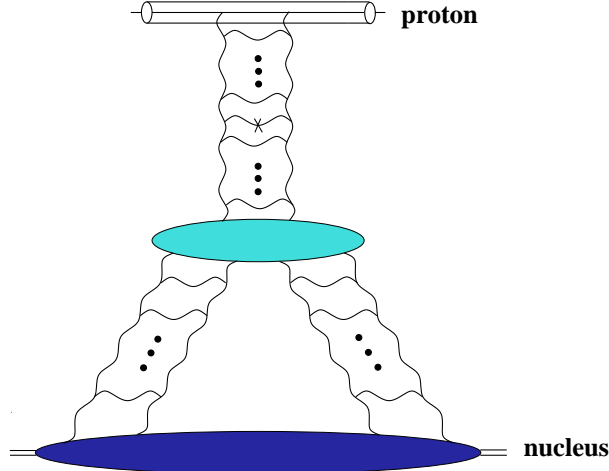


FIG. 7. Gluon production in pA collisions at the next-to-leading twist level (see text). The blob in the center indicates a triple-pomeron vertex.

A perturbative solution of Eq. (41) was constructed in [33] giving the forward amplitude of a $q\bar{q}$ dipole scattering on the nucleus as an expansion in powers of $r_T Q_s(y)$

$$N(\underline{r}, \underline{b}, y) = N_1(\underline{r}, \underline{b}, y) + N_2(\underline{r}, \underline{b}, y) + \dots, \quad (85)$$

where the leading behavior of the n th term in the series is $N_n(\underline{r}, \underline{b}, y) \sim (r_T Q_s(y))^n$. To find the next-to-leading twist correction to the forward scattering amplitude of a gluon dipole N_G we substitute Eq. (85) into Eq. (44) obtaining

$$N_G(\underline{r}, \underline{b}, y) = 2N_1(\underline{r}, \underline{b}, y) + 2N_2(\underline{r}, \underline{b}, y) - [N_1(\underline{r}, \underline{b}, y)]^2 + \dots, \quad (86)$$

where the first term on the right is the leading twist contribution $N_{G1} = 2N_1$ given by Eq. (48), and the next two terms shown in Eq. (86) are the next-to-leading twist corrections. Higher twists are not shown in Eq. (86). To calculate the next-to-leading twist correction to gluon forward amplitude

$$N_{G2}(\underline{r}, \underline{b}, y) = 2N_2(\underline{r}, \underline{b}, y) - [N_1(\underline{r}, \underline{b}, y)]^2 = 2N_2(\underline{r}, \underline{b}, y) - \frac{1}{4} [N_{G1}(\underline{r}, \underline{b}, y)]^2 \quad (87)$$

we use N_{G1} from Eq. (48) and N_2 calculated in [33]. Employing Eq. (23) from [33] in Eq. (9a) from the same reference would give us the first term on the right hand side of Eq. (87). In the end we write for a cylindrical nucleus

$$\begin{aligned}
N_{G2}(r, y) = & -\frac{1}{4} \int \frac{d\lambda_1 d\lambda_2}{(2\pi i)^2} C_{\lambda_1}^A C_{\lambda_2}^A (r_T Q_{s0})^{\lambda_1 + \lambda_2} e^{2\bar{\alpha}_s y [\chi(\lambda_1) + \chi(\lambda_2)]} \\
& \times \left(2^{\frac{\lambda_1 + \lambda_2}{2}} \frac{\Gamma(\frac{\lambda_1}{2}) \Gamma(\frac{\lambda_2}{2}) \Gamma(1 - \frac{\lambda_1 + \lambda_2}{2})}{\Gamma(1 - \frac{\lambda_1}{2}) \Gamma(1 - \frac{\lambda_2}{2}) \Gamma(\frac{\lambda_1 + \lambda_2}{2})} \frac{1}{2[\chi(\lambda_1) + \chi(\lambda_2) - \chi(\lambda_1 + \lambda_2)]} + 1 \right). \quad (88)
\end{aligned}$$

The slight difference between the factors in the integrands of Eq. (88) and Eq. (23) of [33] is due to different definitions of the coefficients C_λ^A (cf. Eq. (15) of [33] with our Eq. (48)).

The first term in the parentheses of Eq. (88) corresponds to the first term on the right hand side of Eq. (87). When we will substitute N_{G2} from Eq. (88) into formula (47) for the cross section, this term would give the contribution illustrated in Fig. 7. It corresponds to the case when the gluon is produced still by the linear evolution with the triple pomeron vertex inserted below the emitted gluon. The rapidity of the triple pomeron vertex was integrated over in arriving at Eq. (88), with only the dominant contribution corresponding to the vertex being right next to the emitted gluon left [33]. (As was shown in [39] the diagrams where the triple pomeron vertex is inserted above the produced gluon cancel in the dipole evolution case considered here [34,32] in agreement with the expectation of the AGK cutting rules [58].) The second term in the parenthesis of Eq. (88) and on the right hand side of Eq. (87) corresponds to the case where the pomeron splitting occurs precisely at the rapidity position of the gluon production. The emitted gluon is produced by the first step of the non-linear evolution. (This term is the main difference between the results of [39] and [40].) As can be seen in the estimates performed below, this term contributes 50% of the answer.

Substituting Eq. (88) in Eq. (47) and integrating over z yields the following contribution to the gluon production cross section at the subleading twist level

$$\begin{aligned}
\frac{d\sigma^{pA}}{d^2 k dy} \Big|_{SLT} = & -\frac{C_F S_p S_A}{\alpha_s 2 (2\pi)^3} \int \frac{d\lambda_1 d\lambda_2 d\lambda'}{(2\pi i)^3} C_{\lambda_1}^A C_{\lambda_2}^A C_{\lambda'}^p \left(\frac{Q_{s0}}{k_T} \right)^{\lambda_1 + \lambda_2} \left(\frac{\Lambda}{k_T} \right)^{\lambda'} \\
& \times e^{2\bar{\alpha}_s y [\chi(\lambda_1) + \chi(\lambda_2)] + 2\bar{\alpha}_s (Y-y) \chi(\lambda')} 2^{\lambda_1 + \lambda_2 + \lambda' - 3} \frac{\Gamma\left(\frac{\lambda_1 + \lambda_2 + \lambda'}{2} - 1\right)}{\Gamma\left(2 - \frac{\lambda_1 + \lambda_2 + \lambda'}{2}\right)} (\lambda_1 + \lambda_2)^2 \lambda'^2 \\
& \times \left(2^{\frac{\lambda_1 + \lambda_2}{2}} \frac{\Gamma(\frac{\lambda_1}{2}) \Gamma(\frac{\lambda_2}{2}) \Gamma(1 - \frac{\lambda_1 + \lambda_2}{2})}{\Gamma(1 - \frac{\lambda_1}{2}) \Gamma(1 - \frac{\lambda_2}{2}) \Gamma(\frac{\lambda_1 + \lambda_2}{2})} \frac{1}{2[\chi(\lambda_1) + \chi(\lambda_2) - \chi(\lambda_1 + \lambda_2)]} + 1 \right). \quad (89)
\end{aligned}$$

To study the onset of higher twist effects, we are interested in the next-to-leading twist contribution (89) in the region of transverse momenta $k_T \gtrsim Q_s(y)$. Performing λ_1 and λ_2 integrations in Eq. (89) around the saddle point (70) and performing the λ' integral in Eq. (89) around the saddle point (58) yields

$$\begin{aligned}
\frac{d\sigma^{pA(2)}}{d^2 k dy} \Big|_{LLA} \approx & -\frac{2 C_F S_p S_A \sqrt{\pi}}{\alpha_s (2\pi)^5} \frac{Q_{s0}^2 \Lambda^2}{k^4} \frac{(C_1^A)^2}{7\zeta(3)} \frac{\ln^{1/4} \frac{k_T}{\Lambda}}{\bar{\alpha}_s y (2\bar{\alpha}_s (Y-y))^{3/4}} \left(\frac{2 \ln \frac{k_T}{Q_{s0}}}{7\zeta(3) \bar{\alpha}_s y} - \sqrt{\frac{2\bar{\alpha}_s (Y-y)}{\ln \frac{k_T}{\Lambda}}} \right) \\
& \times \exp \left[2(\alpha_P - 1)y + 2\sqrt{2\bar{\alpha}_s (Y-y) \ln \frac{k_T}{\Lambda}} - \frac{2 \ln^2 \frac{k_T}{Q_{s0}}}{14\zeta(3) \bar{\alpha}_s y} \right]. \quad (90)
\end{aligned}$$

We do not need to calculate $R^{pA}(k_T, y)$ to see whether the subleading twist correction (90) contributes toward enhancement or suppression. This can be decided by the sign of the contribution (90). The sign of Eq. (90) is determined by the sign of the expression in the parenthesis. One can see that for large k_T the expression in the parenthesis is positive making the overall contribution to the cross section negative, which indicates high- k_T suppression. At lower k_T the sign changes and the term in Eq. (90) begins to contribute toward enhancement of gluon production, signaling the onset of Cronin effect.

The value of k_T at which the transition from suppression to enhancement takes place depends on the rapidity in question as well as on the atomic number A of the nucleus. To estimate the transition value of

k_T one has to equate two terms in the parenthesis of Eq. (90). Assuming that $\ln k_T/Q_{s0} \gg \ln Q_{s0}/\Lambda$ we obtain

$$k_0 \approx k_{\text{geom}} \left(\frac{\Lambda}{Q_{s0}} \right)^{1/3}, \quad (91)$$

with k_{geom} given by Eq. (74). Therefore, the transition from suppression to enhancement in Eq. (90) happens at k_0 which is parametrically smaller than k_{geom} by some powers of A . It is a little worrisome that k_0 is smaller than k_{geom} only by a factor of $A^{-1/18}$, which indicates that the term in Eq. (90) might start contributing toward enhancement of gluon production for k_T still inside the extended geometric scaling region. However this conclusion depends strongly on the definition of extended geometric scaling region: for instance, k_0 is much smaller than k_{geom} given by Eq. (71). One should also note that Eq. (90) gives us a subleading twist contribution which is parametrically smaller than the leading twist term from Eq. (79) in the high- k_T region at hand ($k_T \gtrsim Q_s(y)$). Thus the positive sign of Eq. (90) would, of course, imply that it contributes toward enhancement of gluon production, but it will not guarantee that the contribution of Eq. (90) would overcome the suppression in Eq. (79) to give an overall enhancement of the produced gluons.

We conclude by stating once more that the effect of inclusion of quantum evolution (41) in the gluon production cross section at the next-to-leading twist level is to introduce extra gluon suppression at high k_T , while indicating the onset of Cronin effect by contributing toward gluon enhancement at lower k_T .

D. Toy Model

To illustrate the conclusions reached above let us construct a simple toy model having both Cronin effect and high- k_T suppression in it. We start by modeling the forward amplitude of a gluon dipole scattering on the nucleus by a Glauber-Muller expression from Eq. (9)

$$N_{G\text{ toy}}(\underline{r}, y) = 1 - e^{-\underline{r}^2 Q_{s\text{ toy}}^2(\underline{r}, y)} \quad (92)$$

with the effects of evolution included in the saturation scale. Inspired by Eq. (72), mimicking the double logarithmic approximation (59) we write dropping the prefactors

$$Q_{s\text{ toy}}^2(\underline{r}, y) = Q_{s0}^2 \exp \left(2 \sqrt{2 \bar{\alpha}_s y \ln \frac{1}{r_T Q_{s0}}} \right) \quad (93)$$

with Q_{s0} given by Eq. (18) such that $Q_{s0}^2 = A^{1/3} \Lambda^2$. Our model for $N_{G\text{ toy}}$ given by Eq. (92) includes multiple rescatterings and leading twist evolution effects. The fact that we have chosen double logarithmic approximation for $Q_{s\text{ toy}}^2$ in Eq. (93) implies that we are not including the effects of anomalous dimension (83) which would introduce extra suppression at the leading twist level. Inclusion of higher twists as a Glauber-Mueller multiple rescatterings, while being correct for no-evolution case, is only a model for the fully evolved amplitude and does not capture all the features of Eq. (90).

In the spirit of Eqs. (92) and (93) we write for the gluon dipole–proton amplitude (see also Eq. (33))

$$n_{G\text{ toy}}(\underline{r}, y) = \frac{1}{4} \underline{r}^2 \Lambda_p^2(\underline{r}, y) \ln \frac{1}{r_T \Lambda} \quad (94)$$

with

$$\Lambda_p^2(\underline{r}, y) = \Lambda^2 \exp \left(2 \sqrt{2 \bar{\alpha}_s y \ln \frac{1}{r_T \Lambda}} \right). \quad (95)$$

Substituting Eqs. (92) and (94) into Eq. (47) for a cylindrical nucleus we obtain [cf. Eq. (24)]

$$\left. \frac{d\sigma^{pA}}{d^2 k \, dy} \right|_{\text{toy}} = \frac{\alpha_s C_F S_A}{\pi^2} e^{2\sqrt{2 \bar{\alpha}_s (Y-y) \ln \frac{k_T}{\Lambda}}} \left\{ -\frac{1}{\underline{k}^2} + \frac{2}{\underline{k}^2} e^{-\underline{k}^2/Q_{s\text{ toy}}^2(1/k_T, y)} \right\}$$

$$+ \frac{1}{Q_{s \text{ toy}}^2(1/k_T, y)} e^{-\underline{k}^2/Q_{s \text{ toy}}^2(1/k_T, y)} \left[\ln \frac{Q_{s \text{ toy}}^4(1/k_T, y)}{4 \Lambda^2 \underline{k}^2} + \text{Ei} \left(\frac{\underline{k}^2}{Q_{s \text{ toy}}^2(1/k_T, y)} \right) \right] \} . \quad (96)$$

In arriving at Eq. (96) we assumed that the exponent of the double logarithmic approximation [see Eqs. (93) and (95)] is a slowly varying function of \underline{r} as compared to the factor of \underline{r}^2 in front of it in Eqs. (92) and (94). Therefore, in the spirit of the leading logarithmic approximation we have just replaced $r_T \rightarrow 1/k_T$ in the exponents of Eqs. (93) and (95). Of course the logarithm in Eq. (94) is an even slower varying function of \underline{r} than $\Lambda_p(\underline{r}, y)$, but we did not neglect it since it is needed to reproduce the correct high- k_T asymptotic in Eq. (96). A correct integration also gives the $1/k_T^4$ asymptotic behavior of the gluon production cross section as can be seen from Eq. (59), and the logarithm in Eq. (94) is left there to insure that it also happens in our toy model.

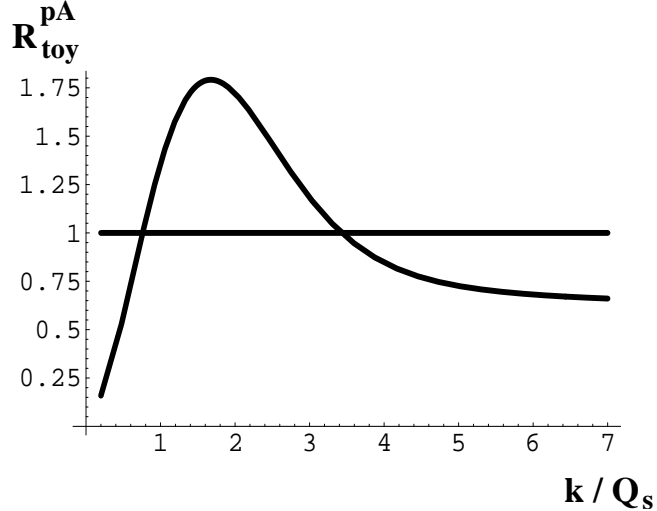


FIG. 8. The ratio R^{pA} plotted as a function of k_T/Q_s for a toy model including multiple rescatterings and mimicking evolution effects. The curve has both Cronin enhancement and high- k_T suppression.

Similar to Eq. (26) we write for the gluon production cross section in pp in the framework of our toy model

$$\frac{d\sigma^{pp}}{d^2k dy} \Big|_{\text{toy}} = \frac{\alpha_s C_F S_p}{\pi^2} e^{2\sqrt{2\bar{\alpha}_s(Y-y)} \ln \frac{k_T}{\Lambda}} \frac{\Lambda_p^2(1/k_T, y)}{\underline{k}^4}. \quad (97)$$

Using Eqs. (96) and (97) in Eq. (25) yields [cf. Eq. (27)]

$$R_{toy}^{pA}(k_T, y) = \frac{\underline{k}^4}{A^{1/3} \Lambda_p^2(1/k_T, y)} \left\{ -\frac{1}{\underline{k}^2} + \frac{2}{\underline{k}^2} e^{-\underline{k}^2/Q_{s \text{ toy}}^2(1/k_T, y)} + \frac{1}{Q_{s \text{ toy}}^2(1/k_T, y)} e^{-\underline{k}^2/Q_{s \text{ toy}}^2(1/k_T, y)} \right. \\ \times \left. \left[\ln \frac{Q_{s \text{ toy}}^4(1/k_T, y)}{4 \Lambda^2 \underline{k}^2} + \text{Ei} \left(\frac{\underline{k}^2}{Q_{s \text{ toy}}^2(1/k_T, y)} \right) \right] \right\}. \quad (98)$$

Our toy model $R^{pA}(k_T, y)$ from Eq. (98) is plotted in Fig. 8 as a function of $k_T/Q_{s \text{ toy}}(\frac{1}{\sqrt{2}} \text{GeV}^{-1}, y = 3)$ for $\Lambda = 0.2 \text{ GeV}$, $y = 3$, $A = 197$ (gold) and $\bar{\alpha}_s = 0.3$. $y = 3$ corresponds to the central rapidity region at RHIC. It exhibits Cronin enhancement due to multiple rescatterings of Eq. (92), as well as high- k_T suppression due to quantum evolution of Eqs. (93) and (95).

V. CONCLUSIONS

In this paper we have demonstrated that the saturation effects in the gluon production in pA at moderate energy can be taken into account in the quasi-classical framework of McLerran-Venugopalan model, which

includes Glauber-Mueller multiple rescatterings, resulting only in Cronin enhancement of produced gluons at $k_T = (1 \div 2) Q_{s0}$, as was shown in Fig. 4 and in Eq. (30). Similar conclusions have been reached in [45,46].

We have also shown that inclusion of quantum evolution introduces suppression of high- k_T gluons produced in pA collisions as compared to the number of gluons produced in pp collisions scaled up by the number of collisions N_{coll} , as suggested previously [7]. There are two distinct sources of high- k_T suppression.

First of all, there are leading twist effects. We have shown how the leading twist suppression arises in the double logarithmic approximation for $k_T > k_{\text{geom}} \gg Q_s(y)$ with the corresponding $R^{pA}(k_T, y)$ given by Eq. (65). At $Q_s(y) < k_T \lesssim k_{\text{geom}}$ the leading twist suppression is mainly due to the change in anomalous dimension λ from its double logarithmic value (57) to the leading logarithmic value (70). $R^{pA}(k_T, y)$ for this k_T -window is given by Eq. (82). This leading twist effect has been originally pointed out in [7]. We have not considered suppression mechanisms that may stem from running of the coupling constant, which would modify the A -dependence of the saturation scale [57].

The second source of high- k_T suppression are the higher twist effects. They become important at $k_T \sim Q_s(y)$. We have calculated the next-to-leading twist correction to the gluon production cross section in pA, which is given by Eq. (90). The correction brings in extra suppression of high- k_T gluon production and starts contributing towards Cronin enhancement at lower k_T .

Evolution-induced high- k_T suppression considered in the paper does not eliminate the Cronin enhancement produced by multiple rescatterings due to the sum rule (38) that we have proven. The position of the Cronin maximum is determined by saturation scale Q_s , while the position of the minimum of high- k_T suppression is given by k_{geom} .

The analysis in the paper was, of course, done for sufficiently high energy and/or rapidity, such that the saturation approach was assumed to be still valid for the highest k_T involved. This implies that the effective Bjorken x is still sufficiently small for all k_T we consider. The extent to which this treatment applies at high k_T hadron production at RHIC is difficult to assess theoretically. We thus eagerly await the results of the experimental analyses of centrality dependence of hadron production above the Cronin region ($k_T \geq 6$ GeV). It is also very important to extend the present measurements away from the central rapidity region to separate initial state effects from possible energy loss in cold nuclear matter. Indeed, in the deuteron fragmentation region, the effects of saturation in the Au wave function will be enhanced, while the density of the produced particles (see, e.g., the predictions in [59]) and thus the associated energy loss will be minimal. In the Au fragmentation region the opposite will be true.

The dAu results will thus allow to clarify the relative importance of initial and final state interactions at different transverse momenta and rapidities of the produced particles. They will be indispensable for establishing a complete physical picture of heavy ion collisions at RHIC energies.

ACKNOWLEDGMENTS

We are greatly indebted to Eugene Levin, Larry McLerran and Alfred Mueller for continuing enjoyable collaborations on the subject. The authors would like to thank Alberto Accardi, Rolf Baier, Miklos Gyulassy, Jamal Jalilian-Marian, Xin-Nian Wang and Urs Wiedemann for stimulating and informative discussions.

The research of D. K. was supported by the U.S. Department of Energy under Contract No. DE-AC02-98CH10886. The work of Yu. K. was supported in part by the U.S. Department of Energy under Grant No. DE-FG03-97ER41014. The work of K. T. was sponsored in part by the U.S. Department of Energy under Grant No. DE-FG03-00ER41132.

- [1] S. S. Adler [PHENIX Collaboration], arXiv:nucl-ex/0306021.
- [2] B. B. Back [PHOBOS Collaboration], arXiv:nucl-ex/0306025.
- [3] J. Adams [STAR Collaboration], arXiv:nucl-ex/0306024.
- [4] K. Adcox *et al.* [PHENIX Collaboration], Phys. Lett. B **561**, 82 (2003) [arXiv:nucl-ex/0207009]; S. S. Adler *et al.* [PHENIX Collaboration], arXiv:nucl-ex/0304022.

[5] B. B. Back *et al.* [PHOBOS Collaboration], collisions at $s(NN)^{**}(1/2) = 200$ -GeV,” arXiv:nucl-ex/0302015.

[6] J. Adams *et al.* [STAR Collaboration], arXiv:nucl-ex/0305015.

[7] D. Kharzeev, E. Levin and L. McLerran, Phys. Lett. B **561**, 93 (2003) [arXiv:hep-ph/0210332].

[8] L. V. Gribov, E. M. Levin and M. G. Ryskin, Phys. Rept. **100**, 1 (1983).

[9] A. H. Mueller and J. w. Qiu, Nucl. Phys. B **268**, 427 (1986).

[10] J. P. Blaizot and A. H. Mueller, Nucl. Phys. B **289**, 847 (1987).

[11] L. D. McLerran and R. Venugopalan, Phys. Rev. D **49**, 2233 (1994) [arXiv:hep-ph/9309289]; Phys. Rev. D **49**, 3352 (1994) [arXiv:hep-ph/9311205]; Phys. Rev. D **50**, 2225 (1994) [arXiv:hep-ph/9402335].

[12] Y. V. Kovchegov, Phys. Rev. D **54**, 5463 (1996) [arXiv:hep-ph/9605446]; Phys. Rev. D **55**, 5445 (1997) [arXiv:hep-ph/9701229]; J. Jalilian-Marian, A. Kovner, L. D. McLerran and H. Weigert, Phys. Rev. D **55**, 5414 (1997) [arXiv:hep-ph/9606337].

[13] J. D. Bjorken, FERMILAB-PUB-82-059-THY (unpublished).

[14] X. N. Wang, M. Gyulassy and M. Plumer, Phys. Rev. D **51**, 3436 (1995) [arXiv:hep-ph/9408344]; M. Gyulassy, P. Levai and I. Vitev, Phys. Rev. Lett. **85**, 5535 (2000) [arXiv:nucl-th/0005032] and references therein.

[15] R. Baier, Y. L. Dokshitzer, A. H. Mueller, S. Peigne and D. Schiff, Nucl. Phys. B **483**, 291 (1997) [arXiv:hep-ph/9607355]; Nucl. Phys. B **484**, 265 (1997) [arXiv:hep-ph/9608322]; R. Baier, Y. L. Dokshitzer, A. H. Mueller and D. Schiff, Phys. Rev. C **58**, 1706 (1998) [arXiv:hep-ph/9803473].

[16] A. Kovner and U. A. Wiedemann, arXiv:hep-ph/0304151 and references therein.

[17] D. Kharzeev and M. Nardi, Phys. Lett. B **507**, 121 (2001) [arXiv:nucl-th/0012025]; D. Kharzeev and E. Levin, Phys. Lett. B **523**, 79 (2001) [arXiv:nucl-th/0108006]; D. Kharzeev, E. Levin and M. Nardi, arXiv:hep-ph/0111315.

[18] J. Schaffner-Bielich, D. Kharzeev, L. D. McLerran and R. Venugopalan, Nucl. Phys. A **705**, 494 (2002) [arXiv:nucl-th/0108048].

[19] Y. V. Kovchegov and K. L. Tuchin, Nucl. Phys. A **708**, 413 (2002) [arXiv:hep-ph/0203213]; Nucl. Phys. A **717**, 249 (2003) [arXiv:nucl-th/0207037].

[20] R. Baier, A. H. Mueller, D. Schiff and D. T. Son, Phys. Lett. B **539**, 46 (2002) [arXiv:hep-ph/0204211].

[21] A. Krasnitz and R. Venugopalan, Phys. Rev. Lett. **84**, 4309 (2000) [arXiv:hep-ph/9909203]; A. Krasnitz and R. Venugopalan, Phys. Rev. Lett. **86**, 1717 (2001) [arXiv:hep-ph/0007108]; A. Krasnitz, Y. Nara and R. Venugopalan, Phys. Rev. Lett. **87**, 192302 (2001) [arXiv:hep-ph/0108092]; A. Krasnitz, Y. Nara and R. Venugopalan, arXiv:hep-ph/0305112.

[22] T. Lappi, Phys. Rev. C **67**, 054903 (2003) [arXiv:hep-ph/0303076].

[23] Y. V. Kovchegov and M. Strikman, Phys. Lett. B **516**, 314 (2001) [arXiv:hep-ph/0107015].

[24] E. Gotsman, E. Levin, U. Maor, L. D. McLerran and K. Tuchin, Nucl. Phys. A **683**, 383 (2001) [arXiv:hep-ph/0007258].

[25] B. Z. Kopeliovich, arXiv:nucl-th/0306044.

[26] Yu. V. Kovchegov and A. H. Mueller, Nucl. Phys. B **529**, 451 (1998) [arXiv:hep-ph/9802440].

[27] B. Z. Kopeliovich, A. V. Tarasov and A. Schafer, Phys. Rev. C **59**, 1609 (1999) [arXiv:hep-ph/9808378].

[28] A. Dumitru and L. D. McLerran, Nucl. Phys. A **700**, 492 (2002) [arXiv:hep-ph/0105268].

[29] A. Kovner and U. A. Wiedemann, Phys. Rev. D **64**, 114002 (2001) [arXiv:hep-ph/0106240].

[30] Y. V. Kovchegov, Nucl. Phys. A **692**, 557 (2001) [arXiv:hep-ph/0011252].

[31] E. A. Kuraev, L. N. Lipatov and V. S. Fadin, Sov. Phys. JETP **45**, 199 (1977) [Zh. Eksp. Teor. Fiz. **72**, 377 (1977)]; I. I. Balitsky and L. N. Lipatov, Sov. J. Nucl. Phys. **28**, 822 (1978) [Yad. Fiz. **28**, 1597 (1978)].

[32] Y. V. Kovchegov, Phys. Rev. D **60**, 034008 (1999) [arXiv:hep-ph/9901281].

[33] Y. V. Kovchegov, Phys. Rev. D **61**, 074018 (2000) [arXiv:hep-ph/9905214].

[34] A. H. Mueller, Nucl. Phys. B **415**, 373 (1994); A. H. Mueller and B. Patel, Nucl. Phys. B **425**, 471 (1994) [arXiv:hep-ph/9403256]; A. H. Mueller, Nucl. Phys. B **437**, 107 (1995) [arXiv:hep-ph/9408245]; Z. Chen and A. H. Mueller, Nucl. Phys. B **451**, 579 (1995).

[35] I. Balitsky, Nucl. Phys. B **463**, 99 (1996) [arXiv:hep-ph/9509348]; arXiv:hep-ph/9706411; Phys. Rev. D **60**, 014020 (1999) [arXiv:hep-ph/9812311].

[36] J. Jalilian-Marian, A. Kovner, A. Leonidov and H. Weigert, Nucl. Phys. B **504**, 415 (1997) [arXiv:hep-ph/9701284]; Phys. Rev. D **59**, 014014 (1999) [arXiv:hep-ph/9706377]; Phys. Rev. D **59**, 034007 (1999) [Erratum-ibid. D **59**, 099903 (1999)] [arXiv:hep-ph/9807462]; J. Jalilian-Marian, A. Kovner and H. Weigert, Phys. Rev. D **59**, 014015 (1999) [arXiv:hep-ph/9709432]; A. Kovner, J. G. Milhano and H. Weigert, Phys. Rev. D **62**, 114005 (2000) [arXiv:hep-ph/0004014]; H. Weigert, Nucl. Phys. A **703**, 823 (2002) [arXiv:hep-ph/0004044].

[37] E. Iancu, A. Leonidov and L. D. McLerran, Nucl. Phys. A **692**, 583 (2001) [arXiv:hep-ph/0011241]; Phys. Lett. B **510**, 133 (2001) [arXiv:hep-ph/0102009]; E. Iancu and L. D. McLerran, Phys. Lett. B **510**, 145 (2001) [arXiv:hep-ph/0103032]; E. Ferreiro, E. Iancu, A. Leonidov and L. McLerran, Nucl. Phys. A **703**, 489 (2002) [arXiv:hep-ph/0109115].

- [38] M. Braun, Eur. Phys. J. C **16**, 337 (2000) [arXiv:hep-ph/0001268].
- [39] Yu. V. Kovchegov and K. Tuchin, Phys. Rev. D **65**, 074026 (2002) [arXiv:hep-ph/0111362].
- [40] M. A. Braun, Phys. Lett. B **483**, 105 (2000) [arXiv:hep-ph/0003003].
- [41] Y. V. Kovchegov, Phys. Rev. D **64**, 114016 (2001) [arXiv:hep-ph/0107256].
- [42] E. Iancu, K. Itakura and L. McLerran, Nucl. Phys. A **708**, 327 (2002) [arXiv:hep-ph/0203137].
- [43] A. H. Mueller, Nucl. Phys. B **335**, 115 (1990).
- [44] J. W. Cronin, H. J. Frisch, M. J. Shochet, J. P. Boymond, R. Mermod, P. A. Piroue and R. L. Sumner, Phys. Rev. D **11**, 3105 (1975).
- [45] B. Z. Kopeliovich, J. Nemchik, A. Schafer and A. V. Tarasov, Phys. Rev. Lett. **88**, 232303 (2002) [arXiv:hep-ph/0201010].
- [46] R. Baier, A. Kovner and U. A. Wiedemann, arXiv:hep-ph/0305265.
- [47] M. G. Ryskin, Yad. Fiz. **32**, 259 (1980); E. M. Levin and M. G. Ryskin, Yad. Fiz. **32**, 802 (1980).
- [48] A. M. Stasto, K. Golec-Biernat and J. Kwiecinski, Phys. Rev. Lett. **86**, 596 (2001) [arXiv:hep-ph/0007192].
- [49] E. Levin and K. Tuchin, Nucl. Phys. B **573**, 833 (2000) [arXiv:hep-ph/9908317].
- [50] L. Frankfurt, G. A. Miller and M. Strikman, Phys. Lett. B **304**, 1 (1993) [arXiv:hep-ph/9305228].
- [51] F. Gelis and J. Jalilian-Marian, Phys. Rev. D **67**, 074019 (2003) [arXiv:hep-ph/0211363].
- [52] M. Anselmino, E. Predazzi, S. Ekelin, S. Fredriksson and D. B. Lichtenberg, Rev. Mod. Phys. **65**, 1199 (1993).
- [53] V. Del Duca, M. E. Peskin and W. K. Tang, Phys. Lett. B **306**, 151 (1993) [arXiv:hep-ph/9303237].
- [54] K. J. Eskola, A. V. Leonidov and P. V. Ruuskanen, Nucl. Phys. B **481**, 704 (1996) [arXiv:hep-ph/9606406].
- [55] V. N. Gribov and L. N. Lipatov, Yad. Fiz. **15**, 781 (1972) [Sov. J. Nucl. Phys. **15**, 438 (1972)]; G. Altarelli and G. Parisi, Nucl. Phys. B **126**, 298 (1977); Y. L. Dokshitzer, (In Russian), Sov. Phys. JETP **46**, 641 (1977) [Zh. Eksp. Teor. Fiz. **73**, 1216 (1977)].
- [56] A. H. Mueller and D. N. Triantafyllopoulos, Nucl. Phys. B **640**, 331 (2002) [arXiv:hep-ph/0205167].
- [57] A. H. Mueller, arXiv:hep-ph/0301109.
- [58] V. A. Abramovsky, V. N. Gribov and O. V. Kancheli, Yad. Fiz. **18** (1973) 595 [Sov. J. Nucl. Phys. **18** (1974) 308].
- [59] D. Kharzeev, E. Levin and M. Nardi, arXiv:hep-ph/0212316.